

An Integrative Analysis of the HD 219134 Planetary System and the Inner Solar System: Extending DYNAMITE with Enhanced Orbital Dynamical Stability Criteria

JEREMY DIETRICH,¹ DÁNIEL APAI,^{1,2} AND RENU MALHOTRA²

¹*Department of Astronomy, The University of Arizona, Tucson, AZ 85721, USA*

²*Lunar and Planetary Laboratory, The University of Arizona, Tucson, AZ 85721, USA*

(Received; Revised; Accepted)

Submitted to AJ

ABSTRACT

Planetary architectures remain unexplored for the vast majority of exoplanetary systems, even among the closest ones, with potentially hundreds of planets still “hidden” from our knowledge. DYNAMITE is a powerful software package that can predict the presence and properties of these yet undiscovered planets. We have significantly expanded the integrative capabilities of DYNAMITE, which now allows for (i) planets of unknown inclinations alongside planets of known inclinations, (ii) population statistics and model distributions for the eccentricity of planetary orbits, and (iii) three different dynamical stability criteria. We demonstrate the new capabilities with a study of the HD 219134 exoplanet system consisting of four confirmed planets and two likely candidates, where five of the likely planets are Neptune-size or below with orbital periods less than 100 days. By integrating the known data for the HD 219134 planetary system with contextual and statistical exoplanet population information, we tested different system architecture hypotheses to determine their likely dynamical stability. Our results provide support for the planet candidates, and we predict at least two additional planets in this system. We also deploy DYNAMITE on analogs of the inner Solar System by excluding Venus or Earth from the input parameters to test DYNAMITE’s predictive power. Our analysis finds the system remains stable while also recovering the excluded planets, demonstrating the increasing capability of DYNAMITE to accurately and precisely model the parameters of additional planets in multi-planet systems.

1. INTRODUCTION

Understanding the stability of planetary systems and searching for a form of order in their dynamics has long been a path of study for astronomers, first for our own Solar System and then in other systems discovered over the past three decades. While we know much about exoplanets as a population, thanks to the transit survey conducted by the Kepler Space Telescope (Borucki et al. 2010) as well as various ground-based radial velocity (RV) surveys, certain questions regarding the dynamical properties of exoplanet systems still remain to this day. The underlying physics is complex and time-consuming to compute mathematically, and astronomers often have to make a compromise between accuracy and speed when modeling these interactions. Still, previ-

ous studies have been able to ascertain simple empirical rules for orbital dynamical stability that fit the known population statistics fairly well (e.g., Pu & Wu 2015; Gilbert & Fabrycky 2020) and detailed computational models that sacrifice speed for more accuracy via N-body integrations, which work well for the analysis of a single, dynamically complicated system (Volk & Malhotra 2020).

The DYNAMITE¹ (Dietrich & Apai 2020) software package provides a unique capability for integrated analysis to combine specific (but often uncertain and incomplete) data of an exoplanet system with population-level statistical information and an empirical rule or other criterion for orbital dynamical stability. This analysis then predicts the presence and parameters of additional “hidden” planets in these planetary systems, which provides

Corresponding author: Jeremy Dietrich
jdietrich1@email.arizona.edu

¹ <https://github.com/JeremyDietrich/dynamite>

enhanced statistical understanding of exoplanet populations. Multiple studies have used DYNAMITE to predict the positions, orbits, and properties (size, nature) of additional planets in dozens of multi-planet systems (e.g., Dietrich & Apai 2020, 2021; Hardegree-Ullman et al. 2021, Basant et al. 2021, submitted). In addition, predictions from DYNAMITE have matched known planets excluded from the analysis, as well as new planets found at the time the integrated analysis was performed (Peterson et al. 2021, submitted). In previous versions of DYNAMITE, we adopted a simple dynamical stability criterion from (He et al. 2019), which was guided by N-body simulations of multi-planet dynamical stability to find that most planet pairs are stable only when their mutual Hill radii is $\gtrsim 8$. However, this criterion, while useful, does not account for some important details - how would the deviation of an orbit from circular along the plane of the system affect the stability? What about orbital resonances with other planets in the system? Which methods to assess stability provide the best mix of accuracy and speed? This paper explores these questions and evaluates three different models of dynamical stability of multi-planet systems.

The HD 219134 system, which is the closest star to the Solar System with at least 6 planets or planet candidates and the closest system with transiting planets (Motalebi et al. 2015; Vogt et al. 2015; Gillon et al. 2017a, hereafter M15; V15; G17), provides a complex, high-multiplicity system on which the various stability analyses can be tested with DYNAMITE. With two planets confirmed to transit by the Transiting Exoplanet Survey Satellite (TESS; Ricker et al. 2015) and two of the other radial velocity signals not fully confirmed by various studies, we can also qualitatively assess support for the candidate planets, along with searching for additional planets that are still unknown. The HD 219134 system will likely be a prime target for direct imaging missions and next-generation ground-based telescopes in the near future, so having a more complete understanding of the planetary system through the predictions we can generate from our DYNAMITE analysis can help guide those observations and instruments.

In addition, the Solar System has provided a great laboratory for analyzing dynamical stability models, including the effects of general relativity on Mercury’s orbit. Thus, as a benchmark, we also deploy DYNAMITE to analyze the results from the stability criteria on the inner Solar System (up to and including Jupiter) as an analog for exoplanet systems, including assessing the system with the exclusion of one of the inner planets. The level of understanding of the Solar System will give strong support on the robustness of our stability mea-

Table 1. Stellar parameters for HD 219134

Parameter Name	Value	Ref.
Spectral Type	K3V	(a)
Mass (M_{\odot})	0.81 ± 0.03	(b)
Radius (R_{\odot})	0.778 ± 0.004	(c)
Luminosity (L_{\odot})	0.265 ± 0.002	(c)
Temperature (K)	4699 ± 16	(c)
Distance (pc)	6.532 ± 0.004	(d)
Rotation period (days)	42.3 ± 0.1	(e)
	22.8 ± 0.03	(f)
Age (Gyr)	11.0 ± 2.2	(b)
	12.46 ± 0.5	(g)

Notes: (a) Gray et al. (2003), (b) G17, (c) Boyajian et al. (2012), (d) Gaia Collaboration et al. (2018), (e) M15, (f) Johnson et al. (2016), (g) Takeda et al. (2007).

asures, as well as continuing to develop the knowledge on how unique the Solar System’s architecture truly is (e.g., Mulders et al. 2018).

This paper is organized as follows. Section 2 discusses the current knowledge of the HD 219134 system, the closest system with 5 or more planets. Section 3 introduces the new features of the DYNAMITE software package. The results of the new analysis on the HD 219134 system are shown in Section 4. Finally, Sections 5-7 discuss the effects of our model assumptions and different parameter tests performed on the HD 219134 system, the dynamical stability criteria evaluated, and their different use cases, and a comparison case via modeling the inner Solar System, including Jupiter.

2. THE HD 219134 SYSTEM

HD 219134 (also known as Gliese 892 or HR 8832) is a main-sequence early-K dwarf, approximately 80% the size of the Sun and about four times less luminous (Gray et al. 2003; Takeda et al. 2007; Boyajian et al. 2012). It is located at a distance of 6.532 ± 0.004 pc from us (Gaia Collaboration et al. 2018), making it one of the 30 closest known planet-hosting stars to our Solar System and the closest to host at least 5 planets. HD 219134 is known to be an impressively old star, with derived age estimates of 11.0 ± 2.2 Gyrs (G17) and 12.46 ± 0.5 Gyrs (Takeda et al. 2007) from various stellar evolution models. The rotation period of the star, via $v \sin i$ measurements and stellar activity measurements taken over 12 years, is likely either $P_{rot} \approx 22.8$ days or $P_{rot} \approx 42.3$ days, relatively short for such an aged star (Johnson et al. 2016; V15; G17). The stellar parameters for HD 219134 can be found in Table 1.

The known system architecture of HD 219134 is illustrated in Figure 1. The first study to detect the presence

HD 219134 System Architecture

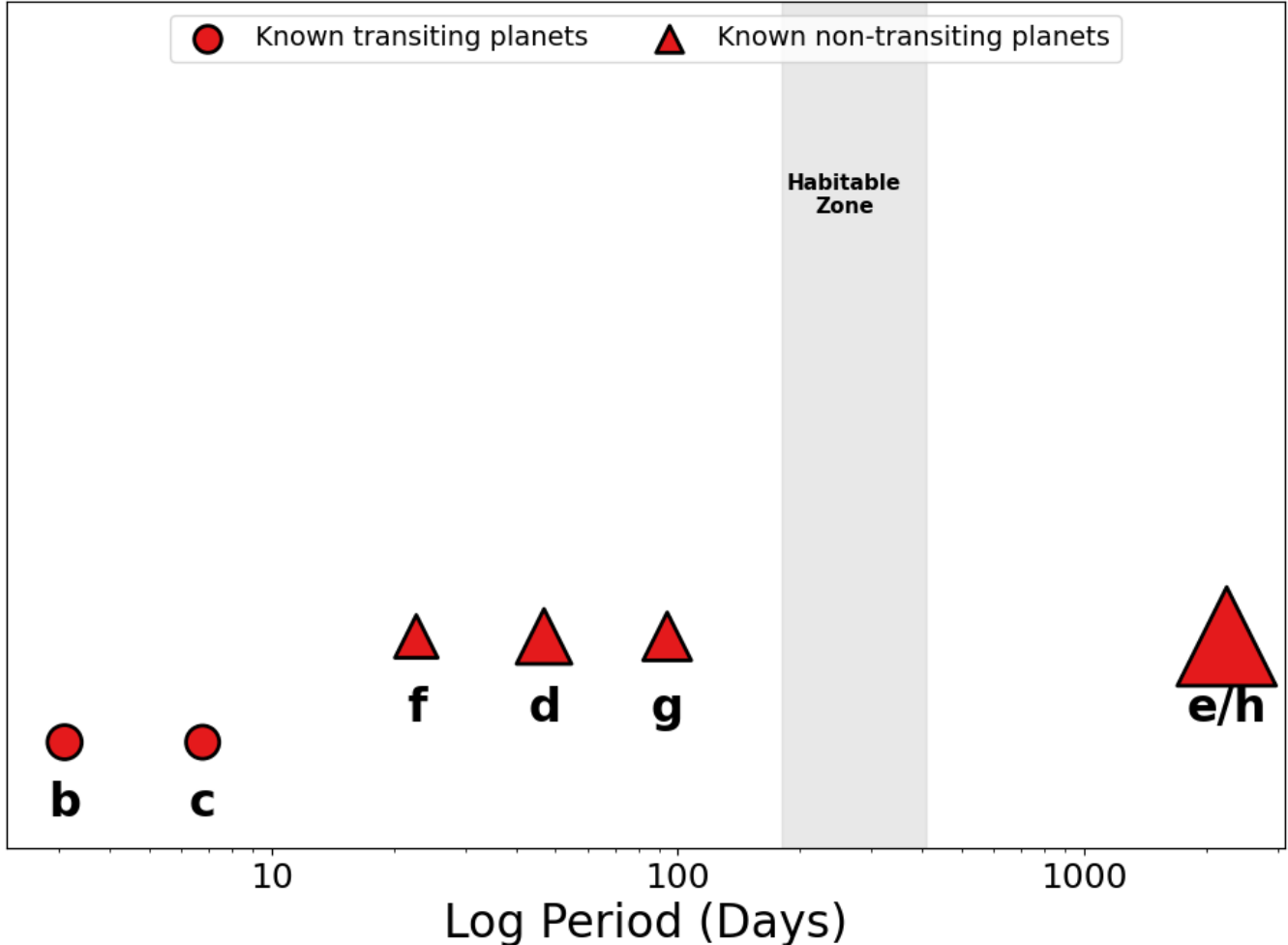


Figure 1. The HD 219134 system architecture with known planets and the extent of the habitable zone. Relative marker sizes match planet sizes. The label “e/h” refers to planet e and planet h likely being the same planet, as they were roughly the same mass but with $\sim 20\%$ difference in orbital periods.

of planets around HD 219134 was done by [M15](#), who found four planets in the system using radial velocity (RV) observations. Three were sub-Neptunian planets located close to the host star with orbital periods of 3.094 (b), 6.767 (c), and 46.66 (d) days, whereas the fourth (e) was a Saturnian or Jovian planet much further out with an orbital period of 1842 days. Shortly thereafter, another RV study by [V15](#) found evidence for six planets in the the system. Notably, they confirmed the presence of planets b-d, discovered evidence for two more sub-Neptunian planets in the inner system at orbital periods of 22.81 (f) and 94.2 (g) days, but did not find planet e; however, they found a similarly massive planet (h) in the outer system, but at a noticeably longer period of 2247 days.

Another study by [Johnson et al. \(2016\)](#), who gathered stellar activity data over a 12 year baseline, found evidence for a rotation period of 22.8 days, while providing no confirmation on the presence of planet f at a very similar orbital period to the rotational/stellar activity period. However, they did confirm planets d and h, stating that planet e was likely a mis-identification of planet h. In addition to their RV observations, [M15](#) also found that planet b transited HD 219134 using photometry from the *Spitzer Space Telescope*. A follow-up transit photometry analysis also using the *Spitzer Space Telescope* by [G17](#) discovered that planet c also transited the host star. This study determined that by geometric probability alone planet c only had a 5.4% chance of transiting the host star, but after confirmation of the

transits of planet b the transiting probability of planet c increased to 21% before it too was found to transit. The observations of planet c transiting, therefore, increase the transit probability of planets f and d to 13% (from 2.5%) and 8.1% (from 1.5%), respectively, as the additional transiting planet means the system inclination is likely closer to edge-on.

TESS observed the HD 219134 system in Sectors 17 and 24 as TOI 1469, and confirmed the transit events for planets b and c but did not detect transits for any other planet². Thus, it is likely that any planets in the inner system with an orbital period within 30 days would either have an inclination far enough away from edge-on such that they would not transit HD 219134 or would be smaller than any known planet in the system. However, due to TESS’s observational strategy, the parameter constraints are not tight for planets with orbital periods longer than TESS’s single-sector observing window of ~ 27 days.

Thus, the presence of planets b-d and e/h have been confirmed in multiple studies, with planet e from the original M15 study found to likely be another manifestation of planet h from V15. The validity of planets f and g (both found by V15) have not yet been established. A recent multi-decade analysis of RV data for the HD 219134 system by Rosenthal et al. (2021) confirmed a signal at $22.795_{-0.006}^{+0.005}$ days that would correspond to planet f, with a slightly smaller $m \sin i$ value. However, they did not report a signal near the originally given period of planet g at ~ 94 days, but analyzed signals near $2\times$ and $4\times$ that period and determined them to be false positives due to annual/instrumental systematics (see Section 5.3).

In our analysis of the HD 219134 system, we do not take the outer gas giant planet e/h (M15; V15) into account, as it is beyond the limits from our current population statistics. Moreover, its existence and properties are inconsistently reported in different studies, as it is not mentioned in any other studies besides these two discovery papers, which have a relatively small but significant inconsistency in the reported values. However, future studies should consider its effects on the inner system and its dynamical stability.

We gathered our information on HD 219134 from the NASA Exoplanet Archive³ and the associated references above. Specifically, the specific data we input to DYNAMITE are only the planet parameters (orbital periods, radii/ $m \sin i$ values, inclination, and eccentricity as well

as their uncertainties) as they are given from the previous studies; we do not re-analyze any of their datasets as there is no reason to do so. A detailed summary of the exoplanet population statistical information is detailed in Dietrich & Apai (2020, 2021), and we only note here that the key trends follow those reported in (Fabrycky et al. 2014; Mulders et al. 2018; He et al. 2019, 2020). In order to provide a complete analysis despite the presence of planets f and g not being well-established in the previous datasets, we also explore the different configurations of the system if planets f and/or g are considered “unconfirmed” and are not included in the system architecture.

3. ANALYSIS

3.1. *The DYNAMITE Software Package*

Here we utilize and expand upon DYNAMITE for our integrated analysis (Dietrich & Apai 2020). We use DYNAMITE to perform a unique integrated analysis of the specific yet incomplete data currently gathered from observations of a system, combined with an orbital dynamical stability criterion for the system and population statistical models for orbital periods, planet radii, inclination, and planet mass-radius relationships. From this analysis, we give predictions on the most likely values for the parameters of one additional planet in the system. Fundamentally, DYNAMITE provides a quantitative answer to the following question: given what we know about the exoplanet population and about this specific planetary system, if there is one yet-undiscovered planet in this system, what are its most likely parameters?

The likelihood distributions for these predictions are derived from the Kepler population of planets (see e.g., Mulders et al. 2018; He et al. 2019, 2020), and the constraints on our predictions are reliant on the prior information given. These priors are gathered from thousands of systems, and therefore are most accurate for systems where the planetary architecture is most similar to those in typical exoplanet systems from the population. If a specific system is exceptional, our predictions may not be accurate and could be contradicted by observations, alerting us to the outlier status of that system. Also, additional priors such as higher precision for data or additional demographic information (e.g., occurrence rate by spectral type, stellar rotational period, etc.) will continue to refine the assumptions in our model (or the specific hypotheses tested) and will adjust our predictions accordingly.

DYNAMITE requires as input the orbital periods and radii or minimum masses and their uncertainties (depending on availability from different types of observations) of the planets, as well as the radius, mass, and

² <https://exofop.ipac.caltech.edu/tess/target.php?id=283722336>

³ <https://exoplanetarchive.ipac.caltech.edu/>

luminosity of the host star. Additional parameters – where unknown values are allowed – include the inclination and eccentricity of the planets. DYNAMITE then calculates the statistical likelihood distributions given the population models (of which there are multiple modules for the different parameters that can be switched and tested separately) and runs a Monte Carlo sampling chain on them. Every set of parameters is tested for dynamical stability and discarded if the system would be considered dynamically unstable (see §3.4 for our new implementation on this consideration).

For ranges in the orbital period distribution that are stable, the likelihood is determined based on the orbital period module chosen. Currently, the two available modules are “equal period ratios”, where planets are most likely to be found when their pairwise period ratios are similar (Mulders et al. 2018), and “clustered periods”, where planets are most likely to be found in clusters with potential gaps in the system (He et al. 2019). We label peaks in the orbital period distribution as significant when $\gtrsim 90\%$ of injections interior to the outermost planet are found in a specific location in the space. We also note positions where multiple planets could exist if we were testing for the presence of more than one additional planet. The output data of DYNAMITE are testable predictions in the form of orbital period, transit depth/probability, RV semi-amplitude, and direct imaging separation and contrast for the planet parameters with the highest likelihood.

The method was originally tested on known Kepler systems with planets removed; such planets were recovered with a good degree of accuracy on the parameters. DYNAMITE was developed on the known TESS multi-planet systems and refined further for analyzing the τ Ceti planetary system, where we predict at least one possibly rocky habitable-zone planet is likely to exist but has not yet been discovered (Dietrich & Apai 2021). Additional studies have utilized DYNAMITE analyses for the K2-138 system with at least 6 planets (Hardegree-Ullman et al. 2021), as well as both Mars in the Solar System and the e Eridani (also known as HD 20794; not to be confused with ϵ Eridani) system of 3 known planets and 3 planet candidates (Basant et al. 2021, submitted). Here we will briefly discuss the objectives of DYNAMITE, in the context of the significant extension of functionalities we added for the present study.

Our goal is to utilize the combined statistical knowledge gathered across all exoplanet systems to determine likelihoods for the presence and properties of planets in specific systems. Our analysis is, therefore, reliant on the accuracy and precision of the data we can gather for a system, as well as our ability to model system param-

eters and orbital stability. We run our analysis in multiple modes with these different modules of data models to assess the accuracy of these models for future analyses and to provide testable hypotheses for models with uncertain levels of knowledge. DYNAMITE has different models for the orbital periods, planet radii, mass-radius relationship, orbital inclination, and orbital eccentricity, and each combination of models provides a different set of predicted planet injections with different likelihoods. The choices made by our analysis are shown in a flowchart in Figure 2. Our motivation to upgrade DYNAMITE and expand its capabilities was to determine the fine structure in dynamical orbital stability, as our previous simple stability model was sufficient for first-approximation results but is likely not a precise model. Here we discuss the updated models and parameter decisions added to DYNAMITE.

3.2. Planet existence hypotheses

We test multiple different hypotheses of the system architecture to determine how incorporating the presence of not-yet-confirmed or uncertain planets and planet candidates changes our understanding of the system architecture and planet properties. Each of these hypotheses is a “branch” on the DYNAMITE data decision tree (see Figure 3) and we explore how these decisions change the results.

In the HD 219134 system, there are two planets with some degree of uncertainty about their existence. Planet f has an orbital period of 22.7 days, which is very close to a measured rotational period for its host star of 22.8 days (Johnson et al. 2016). However, it was included as a known planet for the purpose of updating transit probabilities from the Spitzer follow-up transit study by G17, and a signal with the same period was found over long-term RV data by Rosenthal et al. (2021). Planet g, reported by V15, has no other measurements from any other study; M15 and G17 do not reference it anywhere in their analysis, while Johnson et al. (2016) briefly mention it but do not provide any additional analysis to confirm or reject its existence. The parameter values from the analysis by V15 are much less precise than the other inner planets, but there is no reason to specifically doubt its presence in the system.

For our analysis, we have decided to explore four different system hypotheses in which we include and exclude planet f and planet g from the system architecture, and exclude the outer gas giant planet as stated above. The four hypotheses are defined as below:

- **Hypothesis H[a]:** All five planets b, c, d, f, and g exist at their current parameter values.

Overview of the Extended DYNAMITE Statistical Assessment Process

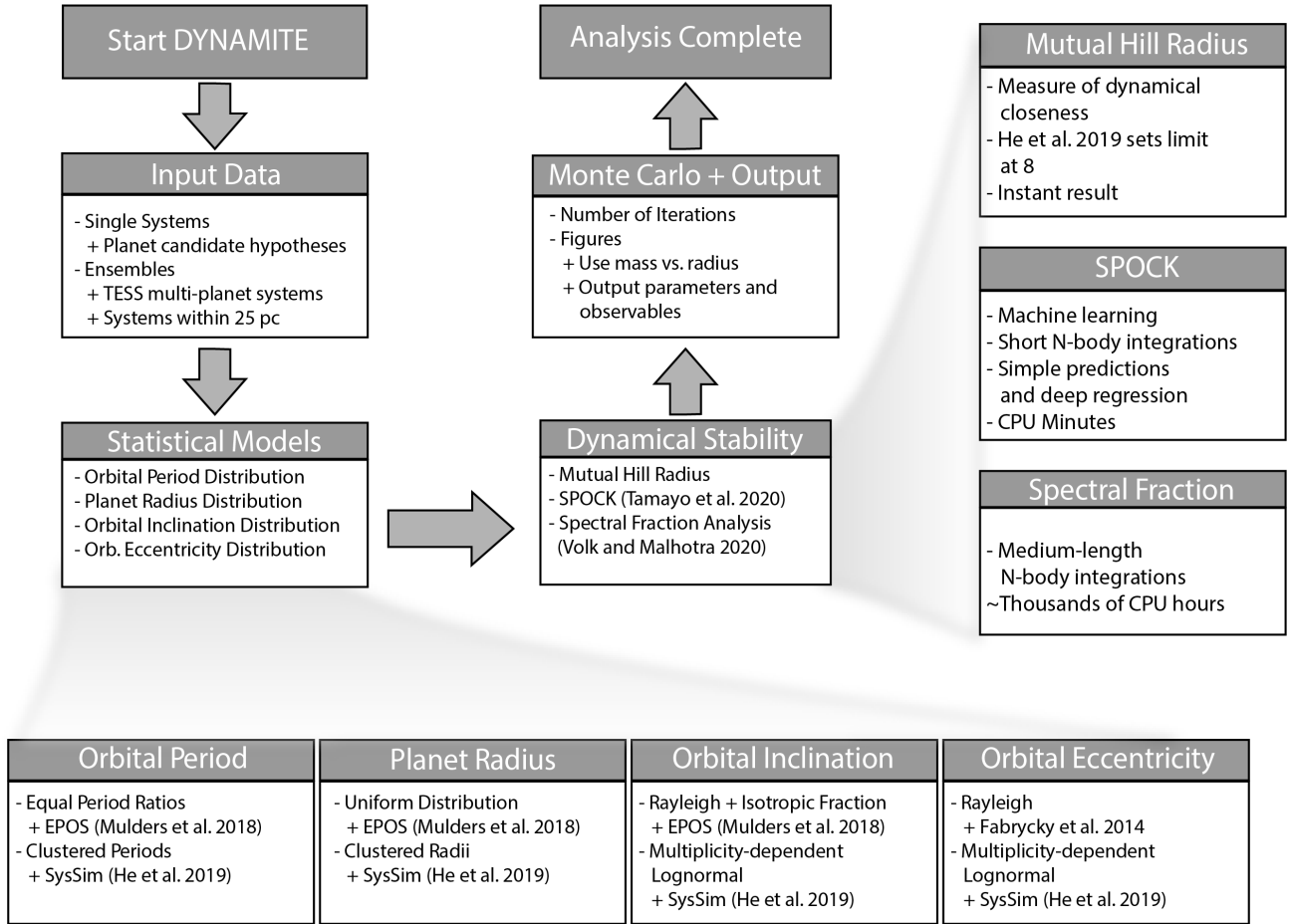


Figure 2. The flowchart of DYNAMITE, with the model choices that are set up in the program’s configuration file.

- **Hypothesis H[b]:** The four planets b, c, d, and f exist, while planet g does not.
- **Hypothesis H[c]:** The four planets b-d and g exist, while planet f does not.
- **Hypothesis H[d]:** The three planets b-d exist, while planets f and g do not.

We treat the excluded planets as “unconfirmed” in our analysis and are not known by the injection algorithm. If the Monte Carlo analysis returns a high relative likelihood at the same orbital periods, we consider this as providing support to the existence of these planets.

3.3. Inclination and eccentricity distributions

We expanded the parameter space available for analysis and refined our modeling by incorporating planets with unknown inclinations and testing two different models for the inclination distribution. For systems where planetary inclinations are unconstrained, our analysis now assumes an isotropic distribution for

the system inclination. For systems where only some planets have inclination constraints, we fit the known values to the requisite distribution of the system inclination for each model described below.

After setting a system inclination (which varies in the isotropic case for each iteration), we distribute the mutual inclinations in two ways. The first model comes from the Exoplanet Populations Observation Simulator (EPOS; Mulders et al. 2018) and assumes a fraction of systems have isotropically-distributed inclinations, while the rest have a narrow ($\sigma_i \sim 2$) Rayleigh distribution of mutual inclinations. The second model comes from the Exoplanets Systems Simulator (SysSim; He et al. 2019, 2020) and assumes a Lognormal distribution with parameters dependent on the multiplicity of the system, where more planets in the system tends to lead to a more coplanar system.

We also included eccentricity distributions, both as another parameter for which we could assess probabilities and as a necessity for the N-body integrations for the

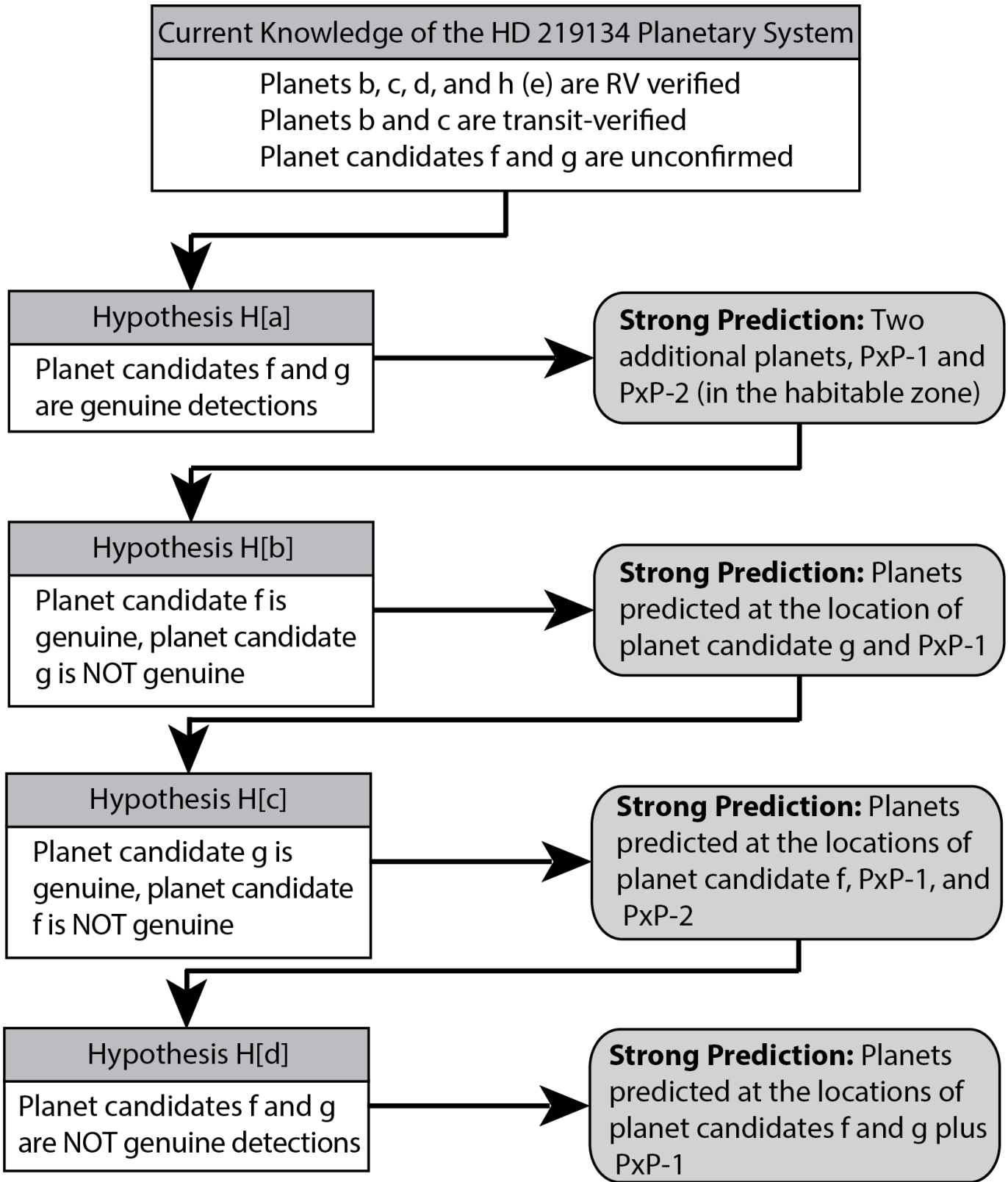


Figure 3. The decision tree of data for DYNAMITE, showing the different hypotheses that can be chosen for the HD 219134 system and can be updated for any given exoplanet system.

dynamical stability criterion (via orbit crossing determinations and AMD measurements). A large fraction of the eccentricities in the Kepler multi-planet system population are $\lesssim 0.1$ (e.g., Xie et al. 2016; Mills et al. 2019; Van Eylen et al. 2019). Our first eccentricity distribution is a Rayleigh distribution with parameter $\sigma_e = 0.02$ (see e.g., Fabrycky et al. 2014), which is not dependent on any other parameter in the system. We also used a multiplicity-dependent Lognormal distribution from SysSim, and as with the inclination model, more planets in the system implies more circular orbits for the planets. For planets without known eccentricities, we sample them from the corresponding distribution for the multiplicity in the system, given that we have injected one planet into the system.

3.4. Dynamical stability

Our goal is to assess the precision of our dynamical stability model and compare the trade-offs required between complexity and speed. The dynamical stability criterion determines the likelihood that the parameters of the predicted planets injected into the system by DYNAMITE do not affect the long-term orbital stability of the other planets in the system and of the injected planet itself. This is an important limiting factor on the injection likelihoods, but it can be a complex and time-consuming process to model. In particular, orbit crossings (i.e., the inner planet of a planet pair having an apastron larger than the periastron of the outer planet in the pair) are not always an indicator of dynamical instability (e.g., in the Solar System the orbits of Neptune and Pluto cross). Here, we make the simplifying assumption that orbital crossings are unstable for planets of similar masses on timescales longer than 1 Gyr, since the reported age of the HD 219134 system is > 10 Gyr. We discuss further the effect of this assumption in Section 6.

The dynamical stability criterion implemented in our previous DYNAMITE analyses was derived from a study by He et al. (2019), who determined that a simple model where planet pairs within 8 mutual Hill radii were unstable and planet pairs outside that value were stable was a good empirical match to current data. However, this criterion did not catch finer details relating to orbital resonances and secular chaos in systems. Therefore, in this study we compare the results from the simple mutual Hill radii cutoff model previously used with two other more detailed analyses involving N-body integrations from Tamayo et al. (2020) and Volk & Malhotra (2020).

First, we test the Stability of Planetary Orbital Configurations Klassifier (SPOCK; Tamayo et al. 2020).

SPOCK utilizes a machine learning algorithm that trains on $1e5$ data sets of planet parameters (both stable and unstable) from N-body integrations and predicts stability using physically motivated summary statistics measured in short N-body integrations ($\sim 10^4$ orbits of innermost planet). This provides a multiple-order-of-magnitude speed-up over full N-body integrations, and thus can be performed within an hour on a single laptop or desktop machine. SPOCK provides both a simple predictor based on a single set of summary features and a deep regression analysis that uses thousands of realizations to better characterize the dynamics of the planetary system. These predictors look at stability of a system as a probabilistic measure instead of the definitive result achieved at the end of the full N-body integration. The level for which a system becomes unstable is where the predictor’s false positive rate hits 10%, which occurs at a stability threshold of 0.34. Tamayo et al. (2020) report that SPOCK provides $\gtrsim 90\%$ accuracy in stability analyses for both predictors, with full N-body simulations being essentially ground truth, and is more accurate in comparison to other stability prediction methods, such as the mutual Hill radius cutoff and the Mean Exponential Growth factor of Nearby Orbits chaos indicator (MEGNO; Cincotta et al. 2003).

Secondly, we test the spectral fraction method from Volk & Malhotra (2020). This analysis performs a medium-length ($\sim 5 \times 10^6$ orbits of innermost planet) N-body integration of the system to determine the likelihood of stability over long N-body integrations ($\sim 5 \times 10^9$ orbits of innermost planet). The spectral fraction is determined by taking the power spectrum of the angular momentum deficit (AMD, a measure of the difference in the orbits from circular and coplanar; see e.g., Laskar & Petit 2017). If a significant fraction of frequencies ($\gtrsim 1\%$) exist at a relatively high percentage of the main peak in the AMD power spectrum ($\gtrsim 5\%$ of the peak), then the system is likely unstable over long ($\sim 5 \times 10^9$ orbits of innermost planet) integrations; otherwise, the system is considered stable.

4. RESULTS

We report the properties of the planets in the HD 219134 system and our predictions for each of our architecture hypotheses, dynamical stability analyses, and statistical model choices in Tables 2-3. The figures showing the relative likelihoods for each hypothesis in two dynamical stability tests are shown in Appendix A, with the mutual Hill radius criterion injections in blue (Figure 11) and the N-body integration injections with the spectral fraction analysis in green (Figure 12). The planet radii are unlikely to be measured via transits for

planets external to planet c due to the inclination of the known planets and the increasingly narrow range of transiting inclinations as the semi-major axis increases. The statistical model choices for the planet radius, inclination, and eccentricity have little effect, whereas the results from each orbital period model (equal period ratios from EPOS (Mulders et al. 2018) and clustered periods from SysSim (He et al. 2019)) and dynamical stability criterion chosen are similar but do show some significant differences. We chose to utilize the equal period ratio orbital period model for our analysis.

4.1. Inclination and eccentricity

We added a new inclination model to test the predictions between them, and also incorporated two different eccentricity models for the dynamical stability analysis that required eccentricities in the N-body integrations. The results from the analysis on the HD 219134 system using the different statistical models are shown in Figure 4. For these results, the other population modules were held constant (equal period ratios, “volatile-rich” M–R relation, and mutual Hill radius stability criterion) to highlight the specific effect of the inclination and eccentricity choices.

The original inclination model, which fits the known mutual inclinations of the system to a Rayleigh distribution with parameter 2° around a central system inclination, found that the transiting planets were likely to be on the “high” side of this mutual inclination distribution, since the remaining planets have not been known to transit. Thus, the system inclination was fit to $\sim 82^\circ$ (where 0° is face-on in the plane of the sky and 90° is edge-on), with the inclination likelihood therefore peaking at 80° and 84° . The new inclination model, which fits the known mutual inclinations of the system to a multiplicity-dependent Lognormal distribution, found unsurprisingly that the system inclination was likely to be near the inclination of the two known transiting planets. This is still consistent with the likelihood of the other known planets not transiting, as the limiting inclination for transits approaches 90° as the orbital period increases. Until additional information is gathered from the system, it is unlikely we will be able to further constrain these parameters.

For the simple model of planet eccentricities, there is no difference between any of the system architecture hypotheses, and so the predictions follow the Rayleigh distribution, with some slight deviations likely due to injections that are rejected due to other parameters. For the multiplicity-dependent Lognormal, we find that higher eccentricities can be expected in general than the Rayleigh distribution, and the mean of the distribution

is higher in Hypothesis H[d] ($\mu = 0.046$) than in Hypothesis H[a] ($\mu = 0.023$). However, none of the models show a high likelihood for having one or multiple planets with moderate eccentricities, as seen in the HD 219134 system.

4.2. Additional planets

Hypothesis H[a]: We find two peaks in the orbital period relative likelihood at ~ 12 days (PxP–1 H[a]) and at ~ 174 days (PxP–2 H[a]). The first peak lies between planet c and planet candidate f, and it can be used to determine the likelihood of planet candidate f being a genuine planet in Hypotheses H[c] and/or H[d] (see Figure 5). The second peak lies beyond planet candidate g and inside the habitable zone of HD 219134, near the inner edge (e.g., Kopparapu et al. 2013). However, as this second peak is an extrapolation beyond the last available data point, the predictions are less constraining in the space beyond the outermost known planet.

Hypothesis H[b]: We again find two peaks in the orbital period likelihood. The first at 12 days corresponds with PxP–1 H[a], which we now call PxP–1 (H[a], H[b]). The second peak, however, moves inward from the peak in Hypothesis H[a], to ~ 90 days. Because planet candidate g has been excluded from the analysis, we now find the peak for PxP–2 H[b] likely corresponds to planet candidate g.

Hypothesis H[c]: Here, the peak around 12 days in the previous hypotheses has been flattened and widened out with the removal of planet candidate f from the analysis. Similar behavior was seen in our past studies (Dietrich & Apai 2020, 2021), where we found evidence that this shape indicates that not one, but two planets are present. When PxP–1 (H[a], H[b]) is added to Hypothesis H[c], we do recover a sharp peak very near the orbital period of planet candidate f, as in Figure 5. Thus, we find this gap could likely hide two planets. The outer peak from Hypothesis H[a] we denoted as PxP–2 H[a] is also visible here, so we update its classification to PxP–2 (H[a], H[c]).

Hypothesis H[d]: We see here the same spread-out pattern between 10 and 30 days indicative of two planets from Hypothesis H[c]. We also find the outer peak has again shifted as in Hypothesis H[b] to a similar position as PxP–2 H[b], so PxP–2 (H[b], H[d]) does provide support for planet candidate g.

4.3. N-body integrations

Our results from the dynamical stability criteria that utilized N-body integrations differed for each of the planet hypotheses. The spectral fraction analysis showed very similar results to the mutual Hill radius,

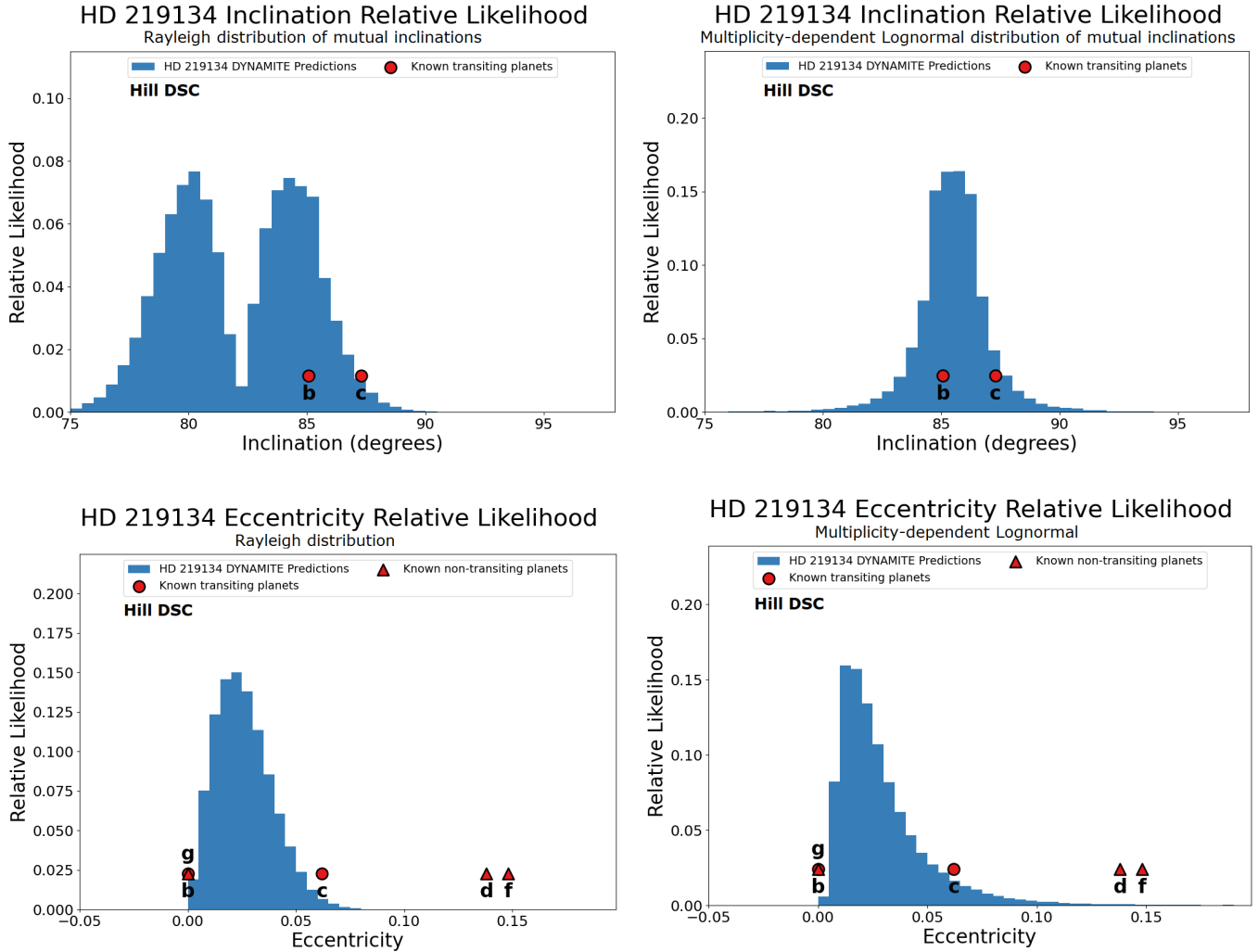


Figure 4. The histograms for the inclinations (top) and eccentricities (bottom) of the predicted injections from DYNAMITE for Hypothesis H[a]; the inclinations for planets b-d are unknown and are therefore not known to the DYNAMITE algorithm nor included in the analysis. The left figures use the Rayleigh + isotropic fraction model for inclinations and Rayleigh model for eccentricities, while the right ones use the multiplicity-dependent Lognormals from the analysis by He et al. (2020). All of the above are using the equal ratios period model, the “volatile-rich” mass-radius relation, and the mutual Hill radius dynamical stability criterion.

even in areas near the mutual Hill radius boundary of 8 (see Figure 12). There were some slight significant differences, including in areas near orbital period resonances, but most of the difference was found to be random noise generated from the Monte Carlo iterations.

SPOCK’s feature classifier finds that the system architectures for Hypotheses H[a]–H[d] would be stable without injecting planets, as the simple stability predictor returns 0.479 ± 0.028 , 0.648 ± 0.036 , 0.636 ± 0.022 , and 0.651 ± 0.023 , respectively, for each of the hypotheses. However, when additional planets are injected via Monte Carlo methods, the system under Hypothesis H[a] is pushed just past the stability limit of 0.34 from predictor (set by the 10% false positive rate), down to 0.328 ± 0.092 . The remaining Hypotheses H[b]–H[d] have

simple stability predictors of 0.868 ± 0.116 , 0.510 ± 0.047 , and 0.910 ± 0.052 , which are all considered stable.

SPOCK’s deep regressor also shows that all four hypotheses as they stand are stable, with the stability predictor having values of 0.407 ± 0.021 , 0.520 ± 0.030 , 0.635 ± 0.020 , and 0.824 ± 0.019 . Adding in another planet to Hypothesis H[a], however, causes the stability predictor to drop to 0.135 ± 0.025 , and no additional planet was considered stable long-term. In addition, injecting a planet in Hypothesis H[b] also drops the stability predictor down to 0.246 ± 0.046 , again with no additional planet found to be stable. For Hypothesis H[c], the stability predictor was 0.349 ± 0.059 over the injection tests, with 60% of the injections accepted as long-term stable. Hypothesis H[d] was stable with re-

Table 2. Planet and Planet Candidate Periods, Radii, and Masses

Name	Period (days)	Radius (R_{\oplus})	Mass (M_{\oplus})	Note	Origin/Reference
HD 219134 b	3.093 ± 0.00001	1.602 ± 0.055	4.74 ± 0.19	Planet	M15; G17
HD 219134 c	6.765 ± 0.0003	1.511 ± 0.047	4.36 ± 0.22	Planet	M15; G17
H[a] PxP-1	12.4 [10.9, 14.7]	1.69 [1.25, 2.27]	3.99 [1.99, 6.36]	Predicted	Ratios, "Volatile", $\Delta = 8$
	12.4 [10.9, 14.5]	1.79 [1.33, 2.41]	6.71 [2.41, 18.7]		Ratios, "Rocky", $\Delta = 8$
	13.3 [10.8, 15.4]	1.68 [1.25, 2.26]	3.95 [1.94, 6.31]		Clustered, "Volatile", $\Delta = 8$
	13.1 [10.7, 15.3]	1.77 [1.32, 2.39]	6.45 [2.34, 18.2]		Clustered, "Rocky", $\Delta = 8$
	12.4 [10.7, 13.7]	1.69 [1.26, 2.28]	3.99 [2.00, 6.40]		Ratios, "Volatile", N-body
	12.4 [10.7, 13.5]	1.79 [1.34, 2.42]	6.71 [2.42, 18.7]		Ratios, "Rocky", N-body
	13.3 [10.6, 15.2]	1.68 [1.26, 2.27]	3.95 [1.95, 6.35]		Clustered, "Volatile", N-body
H[b] PxP-1	12.4 [10.7, 14.4]	1.65 [1.22, 2.22]	3.84 [1.84, 6.14]	Predicted	Ratios, "Volatile", $\Delta = 8$
		1.72 [1.28, 2.31]	5.85 [2.11, 16.2]		Ratios, "Rocky", $\Delta = 8$
	13.3 [10.7, 15.4]	1.65 [1.23, 2.23]	3.84 [1.79, 6.09]		Clustered, "Volatile", $\Delta = 8$
	13.2 [10.7, 15.4]	1.69 [1.27, 2.28]	5.50 [2.05, 15.5]		Clustered, "Rocky", $\Delta = 8$
	12.4 [10.7, 13.9]	1.65 [1.23, 2.23]	3.84 [1.84, 6.18]		Ratios, "Volatile", N-body
		1.72 [1.29, 2.32]	5.85 [2.11, 16.3]		Ratios, "Rocky", N-body
	13.3 [10.7, 15.3]	1.65 [1.24, 2.24]	3.84 [1.79, 6.13]		Clustered, "Volatile", N-body
13.3 [10.7, 15.2]	1.69 [1.28, 2.29]	5.50 [2.05, 15.6]	Clustered, "Rocky", N-body		
H[c] PxP-1	18.1 [14.0, 25.7]	2.13 [1.30, 3.82]	5.75 [2.23, 14.4]	Predicted	Ratios, "Volatile", $\Delta = 8$
	18.1 [13.9, 25.7]	1.77 [1.32, 2.39]	6.45 [2.34, 19.2]		Ratios, "Rocky", $\Delta = 8$
	4.58 [4.38, 4.88]	1.91 [1.25, 3.62]	4.84 [1.95, 13.3]		Clustered, "Volatile", $\Delta = 8$
		1.70 [1.28, 2.30]	5.61 [2.10, 15.9]		Clustered, "Rocky", $\Delta = 8$
	18.1 [14.2, 25.2]	2.14 [1.30, 3.84]	5.79 [2.23, 14.6]		Ratios, "Volatile", N-body
	18.1 [14.1, 25.2]	1.78 [1.32, 2.41]	6.49 [2.34, 19.4]		Ratios, "Rocky", N-body
	4.58 [4.38, 4.88]	1.92 [1.25, 3.63]	4.88 [1.95, 13.5]		Clustered, "Volatile", N-body
1.71 [1.28, 2.32]		5.65 [2.10, 16.0]	Clustered, "Rocky", N-body		
H[d] PxP-1	18.1 [14.4, 25.9]	2.05 [1.29, 4.04]	5.41 [2.17, 15.8]	Predicted	Ratios, "Volatile", $\Delta = 8$
	18.1 [14.5, 25.7]	1.65 [1.22, 2.22]	5.06 [1.83, 14.1]		Ratios, "Rocky", $\Delta = 8$
	4.58 [4.38, 4.88]	1.82 [1.23, 3.66]	4.48 [1.84, 13.5]		Clustered, "Volatile", $\Delta = 8$
		1.59 [1.20, 2.09]	4.46 [1.69, 11.5]		Clustered, "Rocky", $\Delta = 8$
	18.1 [14.2, 25.4]	2.06 [1.29, 4.04]	5.45 [2.17, 15.8]		Ratios, "Volatile", N-body
	18.1 [14.3, 25.2]	1.66 [1.22, 2.22]	5.10 [1.83, 14.1]		Ratios, "Rocky", N-body
	4.58 [4.38, 4.88]	1.83 [1.23, 3.66]	4.52 [1.84, 13.5]		Clustered, "Volatile", N-body
1.60 [1.20, 2.09]		4.50 [1.69, 11.5]	Clustered, "Rocky", N-body		
HD 219134 f	22.72 ± 0.015	Unknown	7.30 ± 0.40	Planet?	M15; G17
HD 219134 d	46.86 ± 0.028	Unknown	16.2 ± 0.64	Planet	M15; G17
HD 219134 g	94.2 ± 0.2	Unknown	11 ± 1	Planet?	V15
H[a] PxP-2	174 [169, 385]	1.69 [1.25, 2.27]	3.99 [1.95, 6.36]	Predicted	Ratios, "Volatile", $\Delta = 8$
	174 [168, 384]	1.79 [1.33, 2.41]	6.71 [2.41, 18.7]		Ratios, "Rocky", $\Delta = 8$
	145 [145, 399]	1.68 [1.25, 2.26]	3.95 [1.94, 6.31]		Clustered, "Volatile", $\Delta = 8$
	145 [145, 393]	1.77 [1.32, 2.39]	6.45 [2.34, 18.2]		Clustered, "Rocky", $\Delta = 8$
	174 [169, 365]	1.69 [1.26, 2.28]	3.99 [2.00, 6.40]		Ratios, "Volatile", N-body
	174 [169, 364]	1.79 [1.34, 2.42]			Ratios, "Rocky", N-body
	145 [145, 381]	1.68 [1.26, 2.27]	3.95 [1.98, 6.35]		Clustered, "Volatile", N-body
145 [145, 376]	1.77 [1.33, 2.41]	6.45 [2.04, 6.43]	Clustered, "Rocky", N-body		

H[b] PxP-2	86.3 [84.8, 206]	1.65 [1.23, 2.23]	3.84 [1.84, 6.18]	Predicted	Ratios, “Volatile”, $\Delta = 8$ Ratios, “Rocky”, $\Delta = 8$ Clustered, “Volatile”, $\Delta = 8$ Clustered, “Rocky”, $\Delta = 8$ Ratios, “Volatile”, N-body Ratios, “Rocky”, N-body Clustered, “Volatile”, N-body Clustered, “Rocky”, N-body			
	86.3 [85.4, 204]	1.72 [1.28, 2.31]	5.85 [2.11, 16.2]					
	73.9 [73.9, 167]	1.65 [1.22, 2.22]	3.84 [1.79, 6.09]					
	74.1 [74.1, 169]	1.70 [1.27, 2.28]	5.61 [2.05, 15.5]					
	86.3 [84.6, 205]	1.65 [1.23, 2.23]	3.84 [1.84, 6.18]					
	86.3 [85.2, 203]	1.72 [1.28, 2.31]	5.85 [2.11, 16.2]					
	73.9 [73.9, 166]	1.65 [1.22, 2.22]	3.84 [1.79, 6.09]					
H[c] PxP-2	174 [169, 386]	2.13 [1.30, 3.81] 1.77 [1.32, 2.38]	5.75 [2.23, 14.4] 6.45 [2.34, 17.9]	Predicted	Ratios, “Volatile”, $\Delta = 8$ Ratios, “Rocky”, $\Delta = 8$ Clustered, “Volatile”, $\Delta = 8$ Clustered, “Rocky”, $\Delta = 8$ Ratios, “Volatile”, N-body Ratios, “Rocky”, N-body Clustered, “Volatile”, N-body Clustered, “Rocky”, N-body			
	141 [140, 389]	1.91 [1.25, 3.62] 1.70 [1.28, 2.30]	4.84 [1.95, 13.3] 5.61 [2.10, 15.9]					
	174 [169, 416]	2.14 [1.30, 3.84] 1.78 [1.32, 2.40]	5.79 [2.23, 14.6] 6.48 [2.34, 18.0]					
	141 [140, 414]	1.92, [1.25, 3.63] 1.71 [1.28, 2.32]	4.87 [1.95, 13.4] 5.63 [2.10, 16.0]					
	H[d] PxP-2	86.3 [85.2, 206]	2.05 [1.29, 4.04]			5.41 [2.17, 15.8]	Predicted	Ratios, “Volatile”, $\Delta = 8$ Ratios, “Rocky”, $\Delta = 8$ Clustered, “Volatile”, $\Delta = 8$ Clustered, “Rocky”, $\Delta = 8$ Ratios, “Volatile”, N-body Ratios, “Rocky”, N-body Clustered, “Volatile”, N-body Clustered, “Rocky”, N-body
		86.3 [85.2, 204]	1.65 [1.23, 2.22]			5.06 [1.83, 14.1]		
		70.2 [69.3, 80.2]	1.82 [1.23, 3.66]			4.48 [1.84, 13.5]		
70.3 [69.3, 80.2]		1.59 [1.20, 2.09]	4.46 [1.69, 11.5]					
86.3 [84.9, 205]		2.06 [1.29, 4.04]	5.45 [2.17, 15.8]					
86.3 [84.9, 203]		1.66 [1.23, 2.23]	5.09 [1.83, 14.1]					
70.2 [69.3, 80.1]		1.83 [1.23, 3.66]	4.52 [1.84, 13.5]					
70.3 [69.3, 80.1]	1.60 [1.20, 2.09]	4.49 [1.69, 11.5]						

Notes: In the PxP naming scheme, H[.] are the different hypotheses as in Section 3.2. Radius is measured for planets b and c, predicted from M–R relationship for remaining planets and predictions. Mass value is given for transit-verified planets b and c as well as predicted planets, whereas $m \sin i$ value is given for RV-verified planets d, f, and g with unknown inclination.

Planets denoted “Planet?” are the two planets that we tested removing from the system. The specific DYNAMITE period model, mass-radius relation, and dynamical stability criterion used are noted in the last column for the predicted planets. The inclination and eccentricity models were fixed as the multiplicity-dependent Lognormals from SysSim (He et al. 2020).

spect to injections with a stability predictor value of 0.473 ± 0.080 .

The N-body integrations did find dips in the relative likelihood near resonances, a feature that is missed by the mutual Hill radius criterion, which is focused more on the space closer to planets. Figure 6 shows the difference between the spectral fraction analysis and the mutual Hill radius for the predicted planets between planets c and f in Hypothesis H[a]. The low-order resonances 2:1 and 3:2 were located at dips in the injections in period space, and additional higher-order resonances 5:3 and 11:6 were added as they coincided with either the same resonance for both planets (11:6) or the 2:1 resonance for the other planet (5:3). The mutual Hill radius criterion does not see this effect.

5. DISCUSSION – DYNAMITE PREDICTIONS

5.1. Inclination and eccentricity distributions

For planets without inclination measurements and $m \sin i$ values measured by radial velocity observations,

the true masses can vary widely due to the assumption of system inclination isotropy, which widens the resulting predicted distribution for the predicted planet mass. For isotropically-distributed inclinations, the potentially large difference in inclination between neighboring planets also affects their dynamical stability in the N-body integrations, decreasing the available space for injecting stable planets between them. Allowing for unknown inclinations provides the most accurate prediction of the likelihood for planet injections, especially when utilizing N-body integrations.

Introducing the eccentricity to the planet parameters for which DYNAMITE tracks in its analysis provides an additional measure in the dynamical stability. While the mutual Hill radius criterion is independent of the eccentricity of the planets, it is easy to determine that a highly eccentric planet would strongly affect the dynamical stability in a way that the mutual Hill radius criterion would be blind to. While it is somewhat unlikely to have highly eccentric planets in higher-multiplicity

Table 3. HD 219134 Planet and Planet Candidate Inclination and Eccentricity

Name	Inclination	Eccentricity	Note	Origin/Reference
HD 219134 b	85.05 ± 0.09	0	Planet	M15; G17
HD 219134 c	87.28 ± 0.10	0.062 ± 0.039	Planet	M15; G17
HD 219134 f	Unknown	0.148 ± 0.047	Planet?	M15; G17
HD 219134 d	Unknown	0.138 ± 0.025	Planet	M15; G17
HD 219134 g	Unknown	0	Planet?	V15
H[a] PxPs	82.0 [79.1, 85.1]	0.024 [0.009, 0.036]	Predicted	Rayleigh+Iso, Rayleigh, $\Delta = 8$
		0.023 [0.012, 0.045]		Rayleigh+Iso, Lognormal, $\Delta = 8$
	85.6 [84.3, 86.7]	0.024 [0.009, 0.036]		Lognormal, Rayleigh, $\Delta = 8$
		0.023 [0.012, 0.045]		Lognormal, Lognormal, $\Delta = 8$
	82.0 [79.2, 85.0]	0.024 [0.009, 0.036]		Rayleigh+Iso, Rayleigh, N-body
		0.023 [0.012, 0.045]		Rayleigh+Iso, Lognormal, N-body
	85.6 [84.4, 86.6]	0.024 [0.009, 0.036]		Lognormal, Rayleigh, N-body
		0.023 [0.012, 0.045]		Lognormal, Lognormal, N-body
H[b] PxPs	82.0 [79.1, 85.1]	0.024 [0.012, 0.039]	Predicted	Rayleigh+Iso, Rayleigh, $\Delta = 8$
		0.031 [0.016, 0.063]		Rayleigh+Iso, Lognormal, $\Delta = 8$
	85.6 [84.1, 87.3]	0.024 [0.012, 0.039]		Lognormal, Rayleigh, $\Delta = 8$
		0.031 [0.016, 0.063]		Lognormal, Lognormal, $\Delta = 8$
	82.0 [79.2, 85.1]	0.024 [0.012, 0.039]		Rayleigh+Iso, Rayleigh, N-body
		0.031 [0.016, 0.063]		Rayleigh+Iso, Lognormal, N-body
	85.6 [84.0, 87.3]	0.024 [0.012, 0.039]		Lognormal, Rayleigh, N-body
		0.031 [0.016, 0.063]		Lognormal, Lognormal, N-body
H[c] PxPs	82.0 [79.1, 85.1]	0.024 [0.012, 0.039]	Predicted	Rayleigh+Iso, Rayleigh, $\Delta = 8$
		0.031 [0.016, 0.063]		Rayleigh+Iso, Lognormal, $\Delta = 8$
	85.6 [84.1, 87.3]	0.024 [0.012, 0.039]		Lognormal, Rayleigh, $\Delta = 8$
		0.031 [0.016, 0.063]		Lognormal, Lognormal, $\Delta = 8$
	82.0 [79.1, 85.0]	0.024 [0.012, 0.039]		Rayleigh+Iso, Rayleigh, N-body
		0.031 [0.016, 0.063]		Rayleigh+Iso, Lognormal, N-body
	85.6 [84.1, 87.2]	0.024 [0.012, 0.039]		Lognormal, Rayleigh, N-body
		0.031 [0.016, 0.063]		Lognormal, Lognormal, N-body
H[d] PxPs	82.7 [78.3, 86.7]	0.024 [0.012, 0.039]	Predicted	Rayleigh+Iso, Rayleigh, $\Delta = 8$
		0.046 [0.023, 0.092]		Rayleigh+Iso, Lognormal, $\Delta = 8$
	86.1 [83.8, 88.6]	0.024 [0.012, 0.039]		Lognormal, Rayleigh, $\Delta = 8$
		0.046 [0.023, 0.092]		Lognormal, Lognormal, $\Delta = 8$
	82.7 [78.3, 86.7]	0.024 [0.012, 0.039]		Rayleigh+Iso, Rayleigh, N-body
		0.046 [0.023, 0.092]		Rayleigh+Iso, Lognormal, N-body
	86.1 [83.8, 88.6]	0.024 [0.012, 0.039]		Lognormal, Rayleigh, N-body
		0.046 [0.023, 0.092]		Lognormal, Lognormal, N-body

Notes: In the PxP naming scheme, H[.] are the different hypotheses for the existence of the known system planets as in Section 3.2. HD 219134 b likely has a tidally circularized orbit due to its semi-major axis, so its eccentricity is set to 0 (G17), and the eccentricity of planet g was set to 0 by V15. Planets denoted “Planet?” are the two planets that we tested removing from the system in the different hypotheses. The specific DYNAMITE inclination and eccentricity models and dynamical stability criterion used are noted in the last column for the predicted planets. The orbital period model and mass-radius relationship were fixed at the period ratios from EPOS (Mulders et al. 2018) and the “volatile-rich” M-R power-law (Otegi et al. 2020)

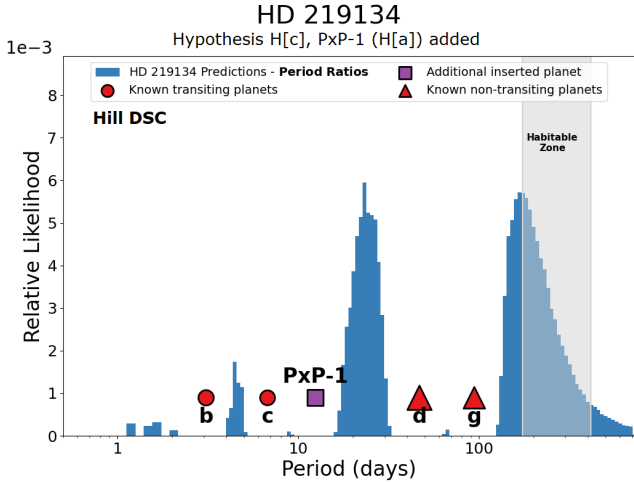


Figure 5. The relative likelihood assuming Hypothesis H[c] for the known planets, but the position of PXP-1 comes from the peak in relative likelihood from Hypothesis H[a]. This shows that the lower and more spread out likelihood of injections seen in Hypotheses H[c] and H[d] is indicative of two potential planets.

systems (e.g., He et al. 2020), our ability to include the eccentricities of the known planets in our predictions helps increase the accuracy of our dynamical stability models and constrain the available parameter space for additional planets.

5.2. Support for planets *f* and *g*

Planet *f*

Based on their RV measurements, V15 detailed the presence of planet *f* at 22.81 days (not found in the analysis by M15), and noted the closeness to the rotational period gathered from $v \sin i$ measurements. By testing different segments of the radial velocity curve for rotational spot modulation residual signals, V15 determined the 22.8-day signal was likely to be real and not a result of the stellar rotation. However, a follow-up analysis by Johnson et al. (2016) narrowed in stellar activity indicators to a period of 22.83 ± 0.03 days, very similar to the reported period of planet *f*. Thus, planet *f* is reported as “controversial” in the NASA Exoplanet Archive, even though a follow-up analysis of the transiting planets by G17 includes planet *f* in its study.

Planet *g*

The analysis by V15 also announced the presence of planet *g* at 94.2 days. This planet was also not found in the fit by M15, and was not even mentioned in the analysis by G17. Johnson et al. (2016) mentioned it in a passing reference to the long rotational period measured via $v \sin i$ by M15, but do not provide any insight into the planet’s existence nor re-assess the data gathered on the planet. Thus, the only data gathered for this planet

come from the V15 study, and the uncertainties on the measured parameters are much larger than the other planets. Still, planet *g* does not hold the “controversial” status that planet *f* has in the Exoplanet Archive, even though its existence is largely centered on only one analysis.

Dynamite analysis

To assess the likelihood of these planets being found at their current positions, we show that if HD 219134 *f* is excluded and a planet is to be added interior to the orbit of planet *d* at 46 days, the period of planet *f* is very near one of two local maxima of the relative likelihood in period space. With no planet *f*, the relative likelihood is spread out between 6 and 46 days. However, if planet *f* is added, then PXP-1 is predicted around 12 days, and conversely if PXP-1 is then added but planet *f* is excluded, we find an additional predicted planet that matches the period of planet *f*. In addition, if HD 219134 *g* is excluded and a planet is to be added exterior to the orbit of planet *d*, the period of planet *g* is very close to the local maximum there as well. Both of these findings are true for the mutual Hill radius cutoff and the N-body integrations; the main difference between them is that the local maximum for planet *g* is pushed slightly further out for the spectral fraction analysis, likely due to the moderately high eccentricity of planet *d*.

5.3. Predicted planets in the HD 219134 system

Depending on the choice of dynamical stability criterion, we predict 1-3 additional planets in the system. We find that an additional planet we label PXP-1 can exist between planets *c* and *f*, with an orbital period of ~ 12 days. If planet *f* is excluded, we find that this single planet likelihood gets stretched in period space and lowered in probability, which we have found is a good indicator that multiple planets can be injected in the gap iteratively (for more details see Dietrich & Apai 2020). Therefore, we find a high probability of recovering planet *f* and still adding PXP-1 around 12 days. This is true for the simple mutual Hill radius dynamical stability criterion as well as both the N-body integration-based SPOCK deep regression and spectral fraction analyses of the HD 219134 system under each system architecture hypothesis.

If planet *g* is excluded from the system we recover it well, and with it in the system we also predict an additional planet PXP-2 with an orbital period of ~ 174 days. This places PXP-2 at the inner edge of the likely habitable zone for HD 219134. If the relatively equal period ratios through the planets (including PXP-1) continues beyond planet *g* through PXP-2, another hypothetical planet could exist with an orbital period of ~ 321

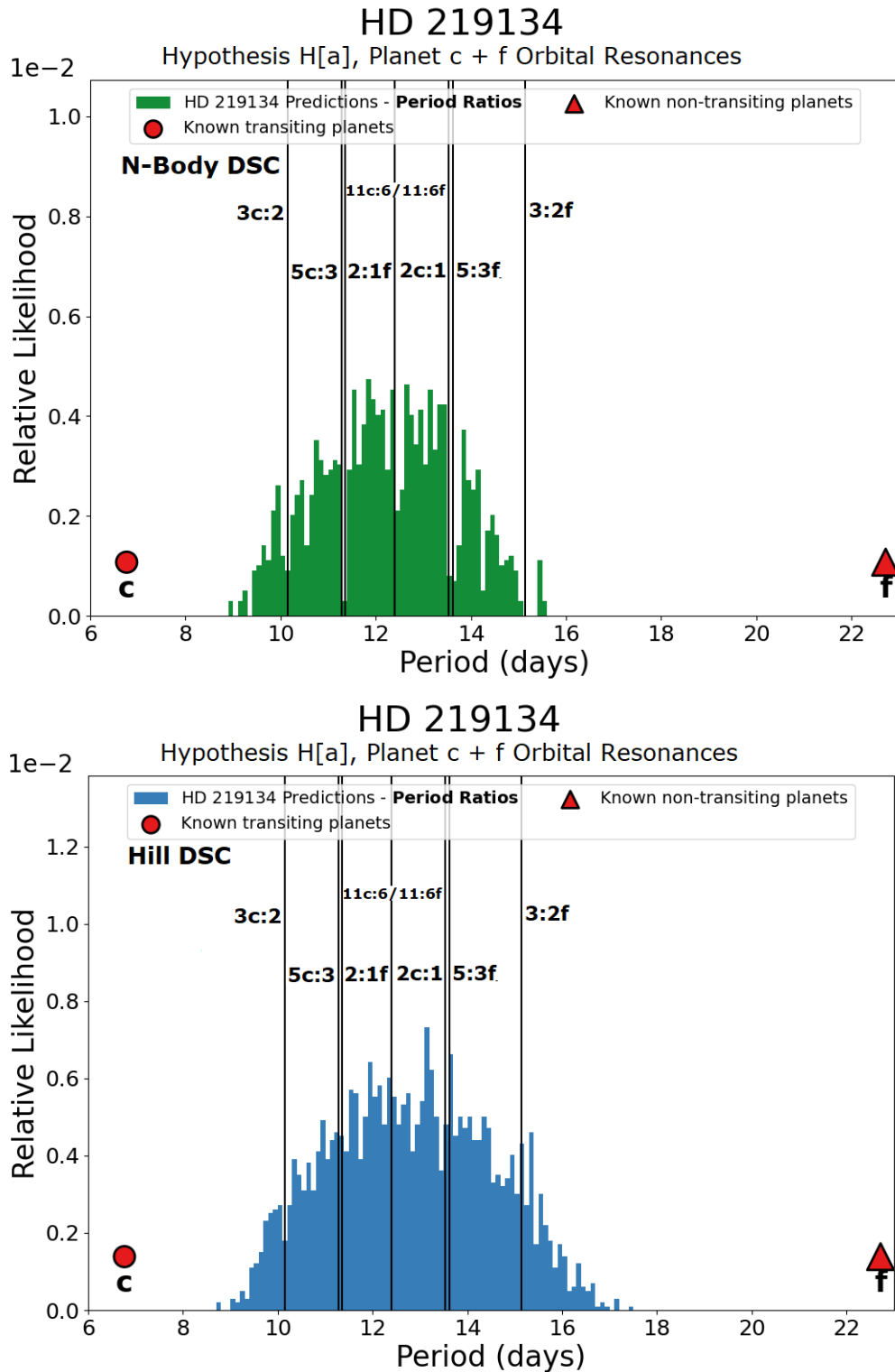


Figure 6. The 2:1, 3:2, 5:3, and 11:6 resonances plotted for an additional planet along with planets c and f in Hypothesis H[a]. 2:1 and 3:2 were chosen as low-order strong resonances, whereas 5:3 and 11:6 are shown because they overlapped a 2:1 resonance or the 11:6 resonance of the other known planet. Top: Injections (in green) via the $\sim 10^6$ -orbit N-body integration dynamical stability criterion, which show lower probabilities of injection near the resonances. Bottom: Injections (in blue) via the mutual Hill radius dynamical stability criterion, which shows no such consistent effect. The difference in y-scale is due to finding fewer planets overall in this gap, as the likelihood gets normalized to 1 across all injections.

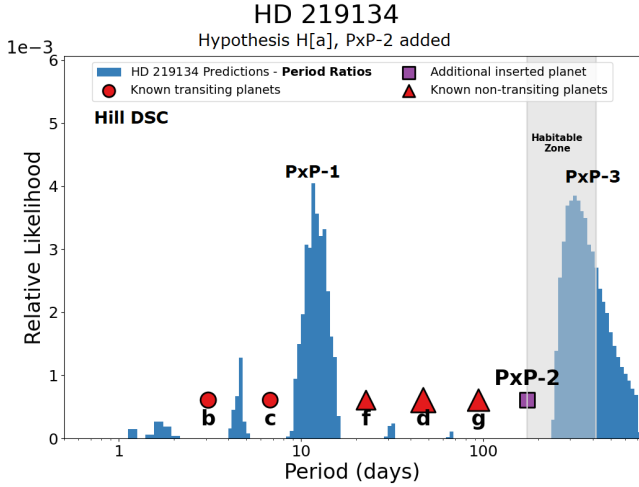


Figure 7. The relative likelihood assuming Hypothesis H[a] for the known planets, but adding in predicted planet Pxp-2 also from Hypothesis H[a], utilizing the mutual Hill radius dynamical stability criterion. This shows an additional predicted planet at around 320 days, in the outer part of the habitable zone.

days, in the outer part of the habitable zone (see Figure 7). This remains true for all of the implementations of the dynamical stability criterion, as the given and expected eccentricities of planet g and Pxp-2 are low, which lessens any effect of the difference between the implementations. We find that an additional planet of $\sim 4 M_{\oplus}$ (near the median of the predicted planet mass distribution) could have an orbital period as close as ~ 140 days and still be stable with respect to planet g, whereas a planet of $\sim 11 M_{\oplus}$ (similar to the masses of the two most exterior planets) could only be located exterior to 150 days and still be stable with respect to planet g.

Rosenthal et al. (2021) reported three false positive radial velocity signals in the HD 219134 system that they attribute to annual and/or instrumental systematics. One of these signals has a period of ~ 28 years, which is close to the entire length of their legacy survey. However, the other two signals are at $192.06^{+0.40}_{-0.49}$ days and $364.3^{+1.9}_{-2.3}$ days. While it is likely that these are false positives from an annual and semi-annual systematic from Earth-based measurements, these signals are relatively close to where we would expect additional planets to exist in this system. The reported respective semi-amplitudes of $2.0^{+0.21}_{-0.20}$ m/s and $1.66^{+0.35}_{-0.31}$ m/s would correspond to $m \sin i$ values of $13.0^{+2.74}_{-2.43} M_{\oplus}$ and $15.7^{+1.64}_{-1.57} M_{\oplus}$, which would lie in between the reported values for planets d and g, the two most massive planets in the inner system and the two furthest out (disregarding the gas giant in the outer system). These values

would either be outside or just inside the 16th-84th percentile range for the predicted mass using the volatile-rich mass-radius relationship (depending on which hypothesis of the system architecture is utilized for the prediction), but would likely still lie within that range for the rocky mass-radius relationship for all system architectures.

6. DISCUSSION – DYNAMICAL STABILITY

Our new dynamical stability criteria utilize N-body integrations to determine the level of stability in a system to a much higher degree of accuracy. However, as using N-body integrations to the standard of 10^9 orbits of the innermost planet is extremely computationally expensive, both of our new models run for shorter integrations (10^4 orbits for SPOCK and 10^6 orbits for the spectral fraction analysis) and predict the likelihood of stability extended out to 10^9 orbits from the results of the short integrations. Whereas the mutual Hill radius measure is essentially instantaneous and thousands of Monte Carlo realizations can be run per second on a standard laptop without utilizing multi-process threads, the N-body integrations need thousands of CPU hours on multiple nodes of a high-performance computer cluster to be run efficiently.

For the N-body analyses, we count Monte Carlo realizations of systems with injections as unstable if they do not survive the initial integration times. SPOCK simply returns a boolean value for the system survival (i.e., without hyperbolic orbits) in the first 10^4 orbits of the innermost planet, but for the spectral fraction analysis we manually reject crossing orbits as well as ejected planets. Figure 8 shows the integration times at which different Monte Carlo realizations of HD 219134 under Hypothesis H[a] went unstable in the N-body integration, as well as showing the spectral fraction analysis for those that survived the initial 10^6 orbits of the innermost planet.

Not all orbital crossings result in prompt planetary collisions and/or ejections (e.g., Neptune and Pluto’s orbits cross). In particular, pairs of similar-mass planets can actually persist in such an unstable configuration for tens to hundreds of Myr timescales if the mutual inclinations between planets are large enough ($\gtrsim 1^\circ$; Rice et al. 2018). However, for the HD 219134 system, the relatively large eccentricities and (likely) mutual inclinations of order $\gtrsim 1^\circ$ would likely cause increasing instability of crossing orbits, and for the ~ 10 Gyr age of this system we would expect most crossing orbits to become unstable on this timescale.

6.1. Mutual Hill radius

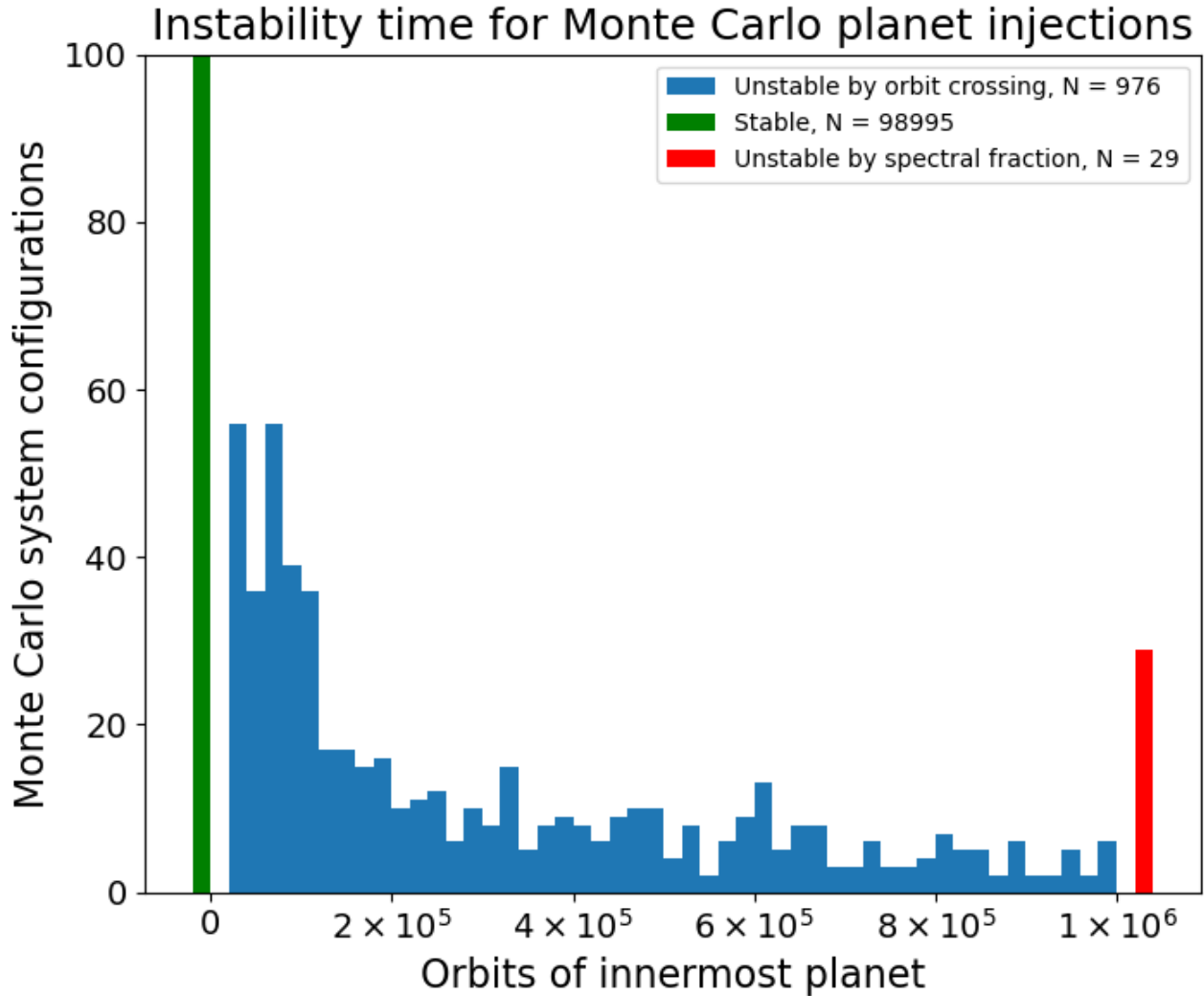


Figure 8. The number of orbits until instability in the N-body integrations for the 10^5 Monte Carlo realizations of the system under Hypothesis H[a]. Almost 99% of the injections were considered stable (green), whereas 29 total integrations were found unstable via spectral fraction analysis after surviving the N-body integration (red).

The mutual Hill radius measure of dynamical closeness has been a predictor of stability for decades (see e.g., Gladman 1993). If a pair of neighboring planets’ semimajor axes are within a certain distance of each other, based on their mass and measured by their Hill spheres of influence, then they will eventually cause the planets to become unstable. This measure provides a simple and fast prediction for any pair of neighboring planets, as the only calculations it requires are basic arithmetic.

The theoretical limit for stability of two-planet systems is that the difference of their semimajor axes (in units of their mutual Hill radius) should not be smaller than $\Delta = 2\sqrt{3} \approx 3.46$. However, there tends to be a distribution in the mutual Hill radius for exoplanet pairs instead of a sharp cutoff (e.g., Malhotra 2015).

In practice, it is found that systems of three or more planets require significantly larger orbital separation of neighboring planets; Pu & Wu (2015) reported $\Delta \gtrsim 12$ for long-term stability of Kepler multis, while Gilbert & Fabrycky (2020) report that a large percentage of known exoplanet systems cluster around $\Delta = 20$. In the present study, we adopted $\Delta = 8$ as a minimum separation, following He et al. (2019). However, there are systems this assessment would classify as unstable that are long-lived due to other considerations (e.g., Kepler-36; Carter et al. 2012), so there are cases when this measure is insufficient. For the HD 219134 system across all of the system architecture hypotheses, we find very little difference between the mutual Hill radius and the other configurations; $\sim 1.1\%$ of injections were found to be

unstable via the Hill radius as compared to $\sim 1.5\%$ for the spectral fraction analysis.

6.2. SPOCK

The utilization of machine learning and training on hundreds of thousands of planetary systems provides a marked improvement in speed over full N-body integrations as well as accuracy over the simpler near-instantaneous methods. SPOCK’s simple feature classifier and deep regressor both perform much faster than the ground-truth full N-body simulations on which they are trained, as well as the spectral fraction analysis, which is performed on integrations 100x longer than SPOCK. SPOCK provides a probabilistic measure of stability for a single system architecture based on the data sets from which it has learned. However, while the training sets attempt to cover as many system architectures as possible, they can cover only a small subset of the uncountable infinity of possible planetary architectures, and therefore it may not provide as accurate of a stability analysis that a full N-body integration could provide.

In our study, SPOCK shows a high level of instability for the more complicated system architecture hypotheses. SPOCK’s FeatureClassifier finds that hypotheses including planet g are shown to be less stable than those where it is excluded, as Hypotheses H[a] and H[c] have stability predictors $\lesssim 0.5$ while H[b] and H[d] are $\gtrsim 0.85$. This suggests that the presence of planet g (and any additional planets beyond it) might negatively affect the stability of the other planets interior to planet g. In addition, the hypotheses including planet f tend to have a higher scatter in the likelihood of stability, as H[a] and H[b] have stability predictor standard deviations of 0.092 and 0.116 as compared to 0.047 and 0.052 for H[c] and H[d]. This likely is a consequence of the moderate reported eccentricity of planet f and the relatively high probability of injecting a planet near 12 days, between planets c and f.

SPOCK’s DeepRegressor provides additional samples of the short N-body integration to determine the probability of stability at a more in-depth level while sacrificing some of its speed. The DeepRegressor showed similar results, with all four system architecture hypotheses stable without any additional planets, albeit with a lower stability predictor than the corresponding FeatureClassifier value. However, adding in another planet to both Hypotheses H[a] and H[b] causes their stability predictors to drop well below the stability threshold, while Hypothesis H[c] remains barely above the value. Hypothesis H[d] is still stable with injections, but its stability predictor is lower than all of the values without

additional planets except for the five-planet architecture in Hypothesis H[a]. In other words, the DeepRegressor finds the HD 219134 system is relatively near the stability limit even with only the three confirmed planets b-d.

In general, if test planets are injected into Hypothesis H[a] anywhere, or into Hypotheses H[b]–H[d] at places that do not specifically correspond to the period of the planet candidates excluded from the analysis of the system, then SPOCK finds the injections would likely cause the system to become unstable (and are therefore rejected). The SPOCK analysis differs from the mutual Hill radius measure and the spectral fraction analysis of HD 219134 in this way, as the other two do not have as large a fraction of rejected injections. In general, SPOCK predicts that the currently known 3-5 planets in the HD 219134 system with orbital periods within 100 days would place the system on the brink of long-term orbital dynamical stability, with little to no room for additional planets.

6.3. Spectral fraction

The spectral fraction analysis is closer to the “ground-truth” of the full N-body integrations with longer test runs, but still provides a usable speed for a system given enough computing resources. This analysis requires ~ 1 CPU hour per 10 Monte Carlo iterations, so the 10^5 iterations used in this analysis took multiple hours on almost a thousand cores of a high-performance computing cluster.

The spectral fraction analysis found results very similar to those from the mutual Hill radius measure, as the injection acceptance rates for each method was 1-2%. In addition, a very small amount of iterations of the system with an additional planet ($\lesssim 5 \times 10^{-4}$) were actually found to be unstable via the empirically-determined threshold values for the spectral fraction from the analysis by Volk & Malhotra (2020). This could likely be a feature of our crossing orbit limit; if a system survives through 10^6 orbits but two planets have crossing orbits that are unstable from spectral fraction, the results count this as unstable via crossing orbits and not from the spectral fraction analysis. If the empirical threshold (1% of the total power spectrum is within 5% of the peak value) is loosened slightly (i.e., 1% of the total power spectrum is within 1% of the peak value, as a majority of the power spectrum is multiple orders of magnitude below the peak), we see a modest increase in the fraction of injections found to be unstable via spectral fraction to $\sim 2 \times 10^{-3}$. Therefore, it is likely that very few injections into the HD 219134 system would allow for secular chaos to cause instabilities that would

be noticeable in the spectral fraction analysis, even for the highest-multiplicity system architecture hypothesis H[a].

However, one significant quantitative difference is the effects of resonances. In particular, in the results from Hypotheses H[a] and H[c] that include planet f, the N-body simulations and spectral fraction analysis find notable drops in the period relative likelihood at both the 2:1 and 3:2 resonances external to planet c and internal to planet f, as well as the overlapping 5:3 (with 2:1) and 11:6 (with itself) resonances. This is consistent with the known pattern in the exoplanet population (e.g., Petrovich et al. 2013; Ramos et al. 2017). However, there are notable examples of multi-planet resonant chains that are stable (e.g., Gillon et al. 2017b; Hardegree-Ullman et al. 2021).

6.4. Lessons Learned on Dynamical Stability Analysis

The mutual Hill radius dynamical stability criterion seems to be a good blend of accuracy and speed. The results are similar to the N-body integration spectral fraction analysis within 0.5% for a very large majority of cases where $\Delta \geq 10$. Furthermore, even running 10^5 Monte Carlo iterations only takes a few seconds on a standard 8-core desktop computer. Thus, in general it would be the likely method of choice for many multi-planet systems.

However, if the system architecture near resonances is being tested, or if there are tightly packed planets where an injection is still deemed likely by the mutual Hill radius criterion, then an N-body integration method would likely be more useful. SPOCK can be utilized to gain a quick understanding of the likely stability of the system before any additional planets are injected. If the value SPOCK reports is near the stability threshold, then the spectral fraction analysis can be performed to determine the stability at a deeper level than the simple model; this requires more computational resources to be available.

For future studies, we will create a hybrid model that chooses which criterion to utilize for a given Monte Carlo iteration of the injected planet parameters. If the distance between planets is within a certain value of the mutual Hill radius (larger than the current limit) or is near a low-order resonance, we would apply a method with N-body integrations. For the majority of Monte Carlo iterations (those that lay outside of the mutual Hill radius and resonance constraints), we would use the simple stability criterion of the mutual Hill radius when adding in the additional planet.

7. DISCUSSION - SOLAR SYSTEM COMPARISON

To compare the results from our different stability criteria for the best-known system, we tested our analysis on a few variants of the inner Solar System to check the performance. We analyzed systems consisting of the terrestrial planets plus Jupiter, and tested excluding Venus or Earth from this group of planets. As for our analysis of HD 219134, we used the period ratios model for the orbital periods, the volatile-rich power-law for the mass-radius relationship, and the SysSim multiplicity-dependent Lognormals for the inclination and eccentricity models. Figure 9 shows the results from this comparison.

We find in this case again that there is very little difference in the mutual Hill radius measure vs the N-body integration methods, as both SPOCK and the spectral fraction analysis agree that the system would be long-term stable even with an additional planet injected. All methods agree that an additional planet would likely be found interior to Mercury (around 35-40 days, given that we are utilizing the equal period ratio model with a constraint on the innermost planet in a system likely being near a 12-day orbit; Mulders et al. 2018), and also between Mars and Jupiter at ~ 1800 days. Of course, this second peak in the relative likelihood roughly corresponds to the location of the asteroid belt in the Solar System, which provides another line of questioning that is beyond the scope of this study: could the location of a predicted planet actually harbor a debris disk or debris ring, and would it be visible in infrared imaging of the system?

When Venus is excluded from the analysis of the inner Solar System, there is an additional large peak in the relative likelihood at ~ 190 days, slightly interior to the actual orbit of Venus at 224 days. When Earth is excluded, there is a large peak at ~ 390 days, slightly exterior to the actual orbit of Earth. Interestingly, in the case where Earth is excluded, all dynamical stability methods predict a small but noticeable probability of injecting a planet between Mercury and Venus at ~ 140 days. However, given the eccentricity of Mercury, it is likely that any planet positioned at this spot in period space could cause Mercury and/or the other planet to become unstable. DYNAMITE also finds significant likelihood of another planet interior to the orbit of Mercury, although less likely than at the orbital period of the planet excluded from the analysis. We do know that there are no planets interior to Mercury, but it is well known that in this aspect the Solar System is atypical (e.g., Mulders et al. 2018); observers from another planetary system who have determined similar exoplanet demographic data to us would likely be surprised to not find a planet within 88 days in the Solar System.

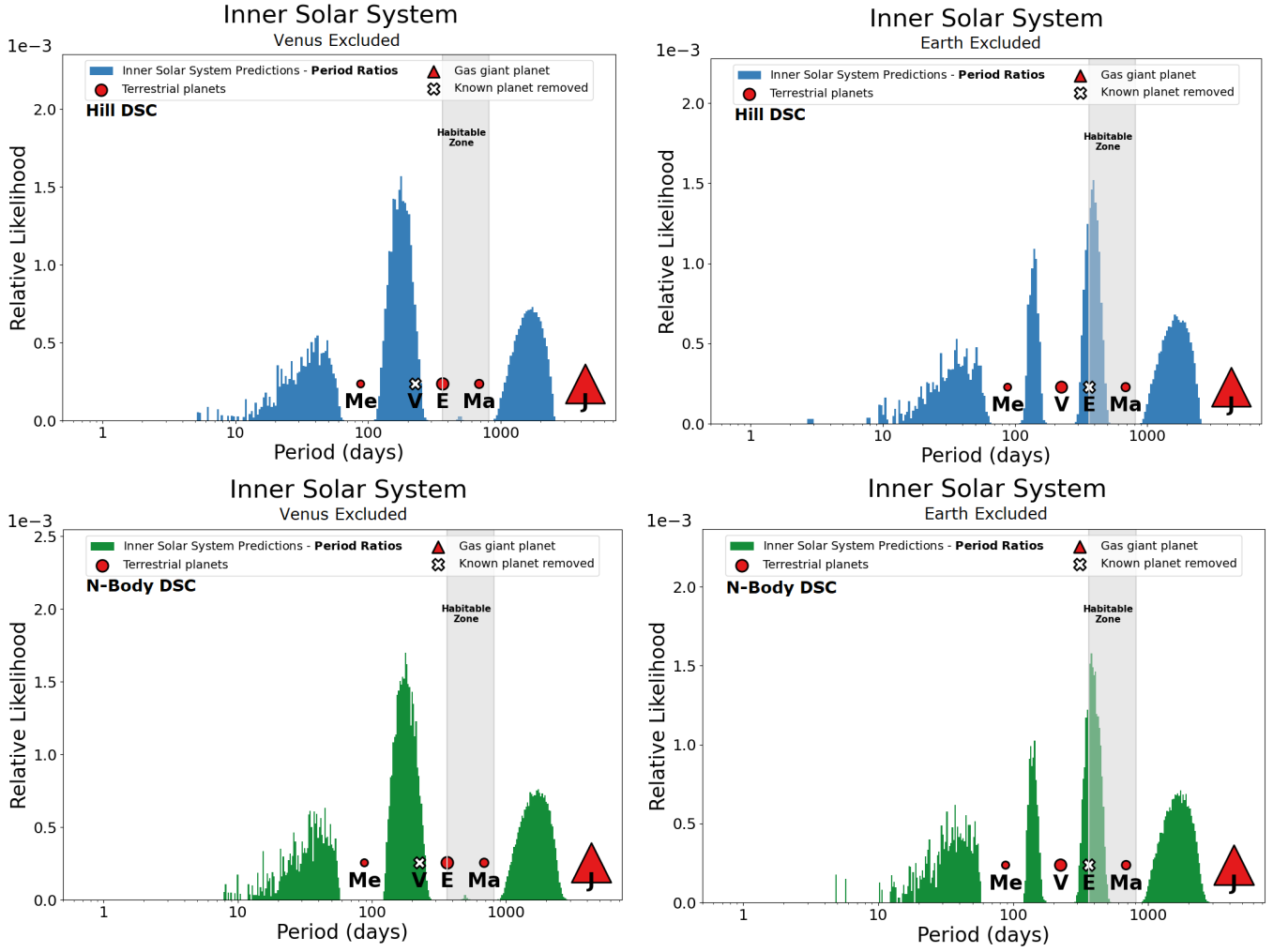


Figure 9. Top: The relative likelihoods in the inner Solar System (+ Jupiter) after removing a planet, utilizing the mutual Hill radius stability criterion. Bottom: The relative likelihoods after removing a planet utilizing the N-body spectral fraction analysis. Left: Venus is excluded from the analysis, showing a large gap where a planet is likely to be located. Right: Earth is excluded from the analysis, showing one prominent gap and one tight gap where a planet could be located. All show a relatively large cumulative probability of a planet in the region of the Solar System occupied by the asteroid belt.

The distribution for the predicted planet radius for additional planets in the Inner Solar System is shown in Figure 10. We find it is well matched to the terrestrial planets, since Jupiter is much larger than the rest of the planets and therefore would not be in the same “cluster” of planet radius via the clustered radius model from SysSim (He et al. 2019). DYNAMITE does find that there would be some probability of finding a planet with a comparatively large physical size, but the main peak in the planet radius distribution is centered on the size of the terrestrial planets.

In conclusion, our analysis is quite successful at predicting the presence of whichever planet is excluded from the inner Solar System, as well as the position of the asteroid belt corresponding to a potential additional planet. While the Solar System is atypical as compared

to the systems in the Kepler population on which our analysis is based (e.g., Mulders et al. 2018), the accurate predictions from DYNAMITE on the Solar System offer another validation of our analysis.

8. SUMMARY

We present an integrated analysis of the HD 219134 planetary system, the closest known 6-planet system, using an updated version of DYNAMITE. The key updates and findings of our study are as follows:

(1) We update and expand the DYNAMITE software by allowing for unknown inclinations in the planet parameter distributions and including measurements of planet eccentricities.

(2) We present advanced dynamical stability criteria (including the inclinations and eccentricities) that utilize N-body integrations. One method uses machine learn-

Inner Solar System Planet Radius Relative Likelihood

Earth Excluded

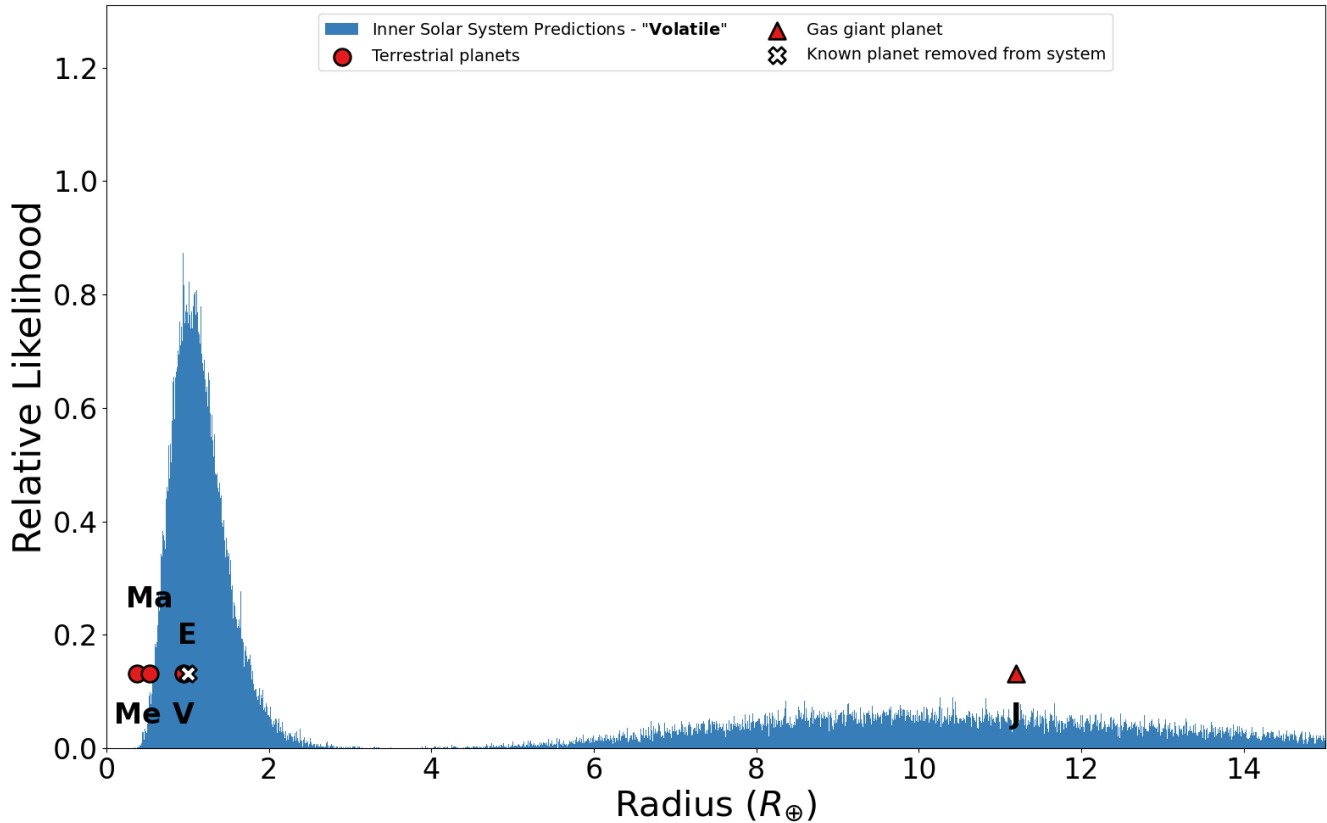


Figure 10. The relative likelihood for an additional planet’s radius in the inner Solar System (+ Jupiter) after removing a planet, utilizing the mutual Hill radius stability criterion. While some probability exists to see a larger planet, the peak is concentrated with the terrestrial planets.

ing to predict stability, and the other performs a “spectral fraction” analysis of the angular momentum deficit (AMD) in the system.

(3) Utilizing both the simple mutual Hill radius dynamical stability criterion and the updated N-body integration spectral fraction analysis, in Hypotheses H[a] and H[c] (where planet f is considered to be real) we find evidence for predicted planet PxP-1 with orbital period ~ 12 days (in between current planets c and f), which would dynamically pack the inner system out to planet g.

(4) Utilizing the same two dynamical stability criteria, in Hypotheses H[b] and H[d] (where planet f is considered to be uncertain) we find a large integrated probability spread out between the peak for PxP-1 in Hypotheses H[a] and H[c] and the expected position of planet f. When PxP-1 is injected at 12 days and run DYNAMITE again, we find that the new injections recover the period of planet f almost exactly.

(5) Using the SPOCK machine-learning predictions, we find that all hypotheses are considered stable with-

out injections, and tends to find that including planet g makes the system more unstable in general, whereas including planet f increases the scatter in the likely stability.

(6) Using the SPOCK simple feature classifier, we find that the dynamical architecture of Hypothesis H[a] is likely fully packed and is likely unstable with any additional planets, while the other hypotheses allow room for additional planets. Using the SPOCK deep regressor predictor, we find Hypotheses H[a] and H[b] are unstable with an additional planet, Hypothesis H[c] is very near the stability limit when injecting a planet, and Hypothesis H[d] is stable with injections.

(7) We find support for both “controversial” planets, planet f with an orbital period of 22.7 days (very near the likely rotation period of its host star) and planet g with an orbital period of 94.2 days (only found in one study of the system through this year, much larger uncertainties).

(8) We also find support for a predicted planet PxP-2 external to the current inner system that would have an

orbital period of ~ 174 days, on the inner edge of the habitable zone, with a likely planet mass of $\sim 4 M_{\oplus}$. Assuming dynamical packing and continuing outwards from there, another planet could be found at an orbital period of ~ 321 days, in the outer parts of the habitable zone. Long-term signals have been found in RV data at ~ 192 days and ~ 364 days, but are found to be more likely to be aliases from Earth’s orbital period (Rosenthal et al. 2021).

(9) We apply this integrated analysis to the inner Solar System up to and including Jupiter, and tested excluding one of the terrestrial planets from the input parameters. Our predictions from the analysis are excellent matches to the known values from the Solar System planets, validating our results.

Our study demonstrates how additional information on dynamical stability can influence the understanding of system architectures and the possibility of finding additional “hidden” planets in these systems. The HD 219134 system, being the closest system to our Sun with 6 planet candidates, was a prime case on which to test our DYNAMITE algorithm’s integrated analysis. We find that dynamically complex systems (i.e., systems with high multiplicity, high eccentricity, etc.) would still allow the presence of another planet without losing dynamical stability. Our study also provides support for the controversial planets/candidates in the HD 219134 system and predictions for additional planets, one of which would lie in the inner part of the habitable zone. This would make HD 219134 an even more enticing tar-

get for direct imaging studies both from space and on the ground in the near future.

ACKNOWLEDGMENTS

The results reported herein benefited from collaborations and/or information exchange within the program “Alien Earths” (supported by the National Aeronautics and Space Administration under Agreement No. 80NSSC21K0593) for NASA’s Nexus for Exoplanet System Science (NExSS) research coordination network sponsored by NASA’s Science Mission Directorate. RM additionally acknowledges funding from NASA grant 80NSSC18K0397. This research has made use of the NASA Exoplanet Archive and the Exoplanet Follow-up Observation Program website, which is operated by the California Institute of Technology, under contract with the National Aeronautics and Space Administration under the Exoplanet Exploration Program. We acknowledge use of the software packages NumPy (Harris et al. 2020), SciPy (Virtanen et al. 2020), Matplotlib (Hunter 2007), and REBOUND (Rein & Liu 2012; Rein et al. 2019). This paper includes data collected by the Kepler mission. Funding for the Kepler mission is provided by the NASA Science Mission Directorate. An allocation of computer time from the UA Research Computing High Performance Computing (HPC) at the University of Arizona is gratefully acknowledged. The citations in this paper have made use of NASA’s Astrophysics Data System Bibliographic Services.

REFERENCES

- Borucki, W. J., Koch, D., Basri, G., et al. 2010, *Science*, 327, 977, doi: [10.1126/science.1185402](https://doi.org/10.1126/science.1185402)
- Boyajian, T. S., von Braun, K., van Belle, G., et al. 2012, *ApJ*, 757, 112, doi: [10.1088/0004-637X/757/2/112](https://doi.org/10.1088/0004-637X/757/2/112)
- Carter, J. A., Agol, E., Chaplin, W. J., et al. 2012, *Science*, 337, 556, doi: [10.1126/science.1223269](https://doi.org/10.1126/science.1223269)
- Cincotta, P. M., Giordano, C. M., & Simó, C. 2003, *Physica D Nonlinear Phenomena*, 182, 151, doi: [10.1016/S0167-2789\(03\)00103-9](https://doi.org/10.1016/S0167-2789(03)00103-9)
- Dietrich, J., & Apai, D. 2020, *AJ*, 160, 107, doi: [10.3847/1538-3881/aba61d](https://doi.org/10.3847/1538-3881/aba61d)
- . 2021, *AJ*, 161, 17, doi: [10.3847/1538-3881/abc560](https://doi.org/10.3847/1538-3881/abc560)
- Fabrycky, D. C., Lissauer, J. J., Ragozzine, D., et al. 2014, *ApJ*, 790, 146, doi: [10.1088/0004-637X/790/2/146](https://doi.org/10.1088/0004-637X/790/2/146)
- Gaia Collaboration, Brown, A. G. A., Vallenari, A., et al. 2018, *A&A*, 616, A1, doi: [10.1051/0004-6361/201833051](https://doi.org/10.1051/0004-6361/201833051)
- Gilbert, G. J., & Fabrycky, D. C. 2020, *AJ*, 159, 281, doi: [10.3847/1538-3881/ab8e3c](https://doi.org/10.3847/1538-3881/ab8e3c)
- Gillon, M., Demory, B.-O., Van Grootel, V., et al. 2017a, *Nature Astronomy*, 1, 0056, doi: [10.1038/s41550-017-0056](https://doi.org/10.1038/s41550-017-0056)
- Gillon, M., Triaud, A. H. M. J., Demory, B.-O., et al. 2017b, *Nature*, 542, 456, doi: [10.1038/nature21360](https://doi.org/10.1038/nature21360)
- Gladman, B. 1993, *Icarus*, 106, 247, doi: [10.1006/icar.1993.1169](https://doi.org/10.1006/icar.1993.1169)
- Gray, R. O., Corbally, C. J., Garrison, R. F., McFadden, M. T., & Robinson, P. E. 2003, *AJ*, 126, 2048, doi: [10.1086/378365](https://doi.org/10.1086/378365)
- Hardegree-Ullman, K. K., Christiansen, J. L., Ciardi, D. R., et al. 2021, *AJ*, 161, 219, doi: [10.3847/1538-3881/abeab0](https://doi.org/10.3847/1538-3881/abeab0)
- Harris, C. R., Millman, K. J., van der Walt, S. J., et al. 2020, *Nature*, 585, 357–362, doi: [10.1038/s41586-020-2649-2](https://doi.org/10.1038/s41586-020-2649-2)
- He, M. Y., Ford, E. B., & Ragozzine, D. 2019, *MNRAS*, 490, 4575, doi: [10.1093/mnras/stz2869](https://doi.org/10.1093/mnras/stz2869)
- He, M. Y., Ford, E. B., Ragozzine, D., & Carrera, D. 2020, *AJ*, 160, 276, doi: [10.3847/1538-3881/abba18](https://doi.org/10.3847/1538-3881/abba18)

- Hunter, J. D. 2007, *Computing in Science and Engineering*, 9, 90, doi: [10.1109/MCSE.2007.55](https://doi.org/10.1109/MCSE.2007.55)
- Johnson, M. C., Endl, M., Cochran, W. D., et al. 2016, *ApJ*, 821, 74, doi: [10.3847/0004-637X/821/2/74](https://doi.org/10.3847/0004-637X/821/2/74)
- Kopparapu, R. K., Ramirez, R., Kasting, J. F., et al. 2013, *ApJ*, 765, 131, doi: [10.1088/0004-637X/765/2/131](https://doi.org/10.1088/0004-637X/765/2/131)
- Laskar, J., & Petit, A. C. 2017, *A&A*, 605, A72, doi: [10.1051/0004-6361/201630022](https://doi.org/10.1051/0004-6361/201630022)
- Malhotra, R. 2015, *ApJ*, 808, 71, doi: [10.1088/0004-637X/808/1/71](https://doi.org/10.1088/0004-637X/808/1/71)
- Mills, S. M., Howard, A. W., Petigura, E. A., et al. 2019, *AJ*, 157, 198, doi: [10.3847/1538-3881/ab1009](https://doi.org/10.3847/1538-3881/ab1009)
- Motalebi, F., Udry, S., Gillon, M., et al. 2015, *A&A*, 584, A72, doi: [10.1051/0004-6361/201526822](https://doi.org/10.1051/0004-6361/201526822)
- Mulders, G. D., Pascucci, I., Apai, D., & Ciesla, F. J. 2018, *AJ*, 156, 24, doi: [10.3847/1538-3881/aac5ea](https://doi.org/10.3847/1538-3881/aac5ea)
- Otegi, J. F., Bouchy, F., & Helled, R. 2020, *A&A*, 634, A43, doi: [10.1051/0004-6361/201936482](https://doi.org/10.1051/0004-6361/201936482)
- Petrovich, C., Malhotra, R., & Tremaine, S. 2013, *ApJ*, 770, 24, doi: [10.1088/0004-637X/770/1/24](https://doi.org/10.1088/0004-637X/770/1/24)
- Pu, B., & Wu, Y. 2015, *ApJ*, 807, 44, doi: [10.1088/0004-637X/807/1/44](https://doi.org/10.1088/0004-637X/807/1/44)
- Ramos, X. S., Charalambous, C., Benítez-Llambay, P., & Beaugé, C. 2017, *A&A*, 602, A101, doi: [10.1051/0004-6361/201629642](https://doi.org/10.1051/0004-6361/201629642)
- Rein, H., & Liu, S. F. 2012, *A&A*, 537, A128, doi: [10.1051/0004-6361/201118085](https://doi.org/10.1051/0004-6361/201118085)
- Rein, H., Hernandez, D. M., Tamayo, D., et al. 2019, *MNRAS*, 485, 5490, doi: [10.1093/mnras/stz769](https://doi.org/10.1093/mnras/stz769)
- Rice, D. R., Rasio, F. A., & Steffen, J. H. 2018, *MNRAS*, 481, 2205, doi: [10.1093/mnras/sty2418](https://doi.org/10.1093/mnras/sty2418)
- Ricker, G. R., Winn, J. N., Vanderspek, R., et al. 2015, *Journal of Astronomical Telescopes, Instruments, and Systems*, 1, 014003, doi: [10.1117/1.JATIS.1.1.014003](https://doi.org/10.1117/1.JATIS.1.1.014003)
- Rosenthal, L. J., Fulton, B. J., Hirsch, L. A., et al. 2021, *ApJS*, 255, 8, doi: [10.3847/1538-4365/abe23c](https://doi.org/10.3847/1538-4365/abe23c)
- Takeda, G., Ford, E. B., Sills, A., et al. 2007, *ApJS*, 168, 297, doi: [10.1086/509763](https://doi.org/10.1086/509763)
- Tamayo, D., Cranmer, M., Hadden, S., et al. 2020, *Proceedings of the National Academy of Science*, 117, 18194, doi: [10.1073/pnas.2001258117](https://doi.org/10.1073/pnas.2001258117)
- Van Eylen, V., Albrecht, S., Huang, X., et al. 2019, *AJ*, 157, 61, doi: [10.3847/1538-3881/aaf22f](https://doi.org/10.3847/1538-3881/aaf22f)
- Virtanen, P., Gommers, R., Oliphant, T. E., et al. 2020, *Nature Methods*, 17, 261, doi: [10.1038/s41592-019-0686-2](https://doi.org/10.1038/s41592-019-0686-2)
- Vogt, S. S., Burt, J., Meschiari, S., et al. 2015, *ApJ*, 814, 12, doi: [10.1088/0004-637X/814/1/12](https://doi.org/10.1088/0004-637X/814/1/12)
- Volk, K., & Malhotra, R. 2020, *AJ*, 160, 98, doi: [10.3847/1538-3881/aba0b0](https://doi.org/10.3847/1538-3881/aba0b0)
- Xie, J.-W., Dong, S., Zhu, Z., et al. 2016, *Proceedings of the National Academy of Science*, 113, 11431, doi: [10.1073/pnas.1604692113](https://doi.org/10.1073/pnas.1604692113)

APPENDIX

A. DYNAMITE INJECTION FIGURES

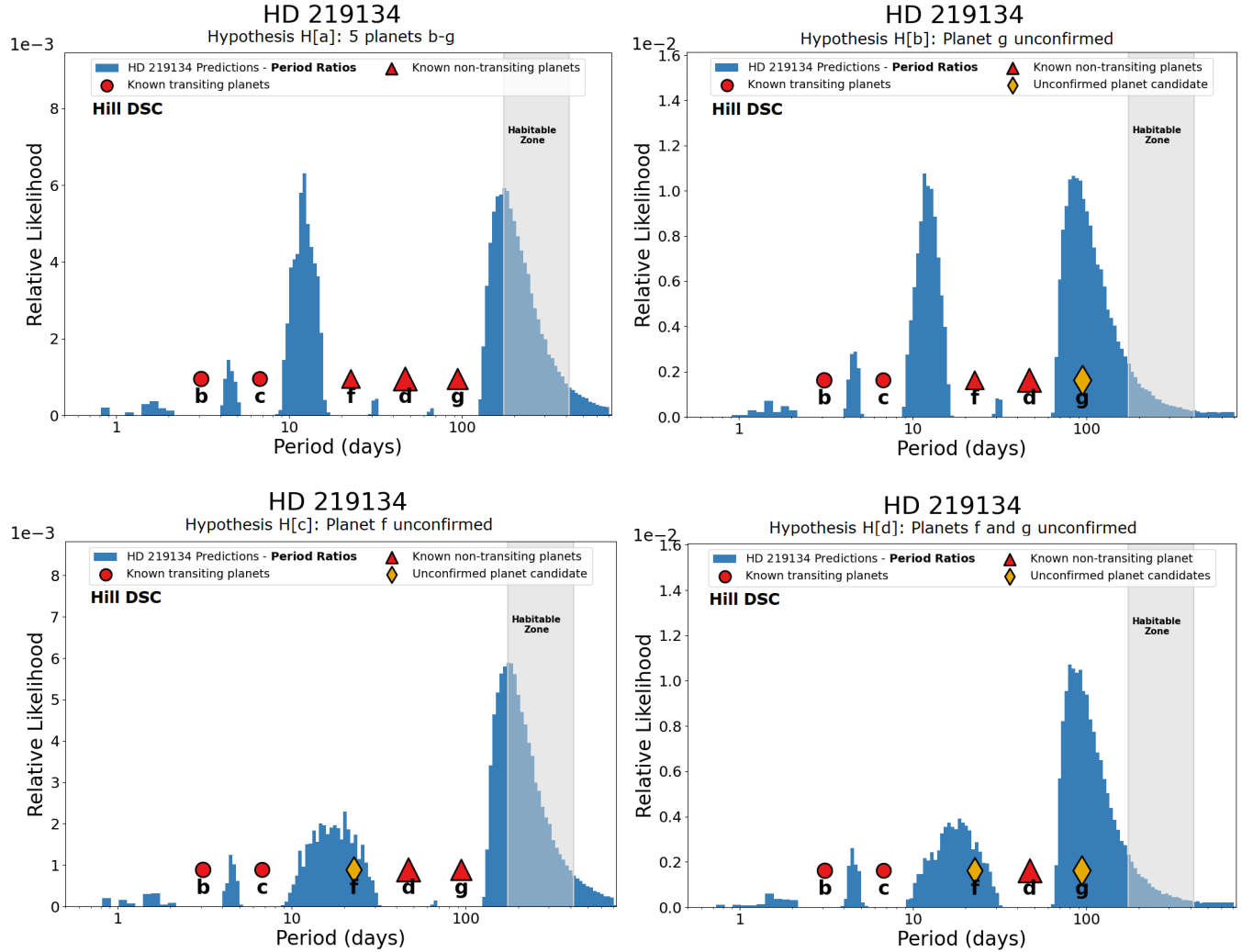


Figure 11. DYNAMITE analysis utilizing the simple dynamical stability criterion requiring neighboring planets' separation in semimajor axis to exceed 8 mutual Hill radii. Top left: Analysis assuming Hypothesis a, the full 5-planet system. Top right: Analysis assuming Hypothesis b, with no planet f (orbital period near stellar rotation period). Bottom left: Analysis assuming Hypothesis c, with no planet g (not found in all studies). Bottom right: Analysis assuming Hypothesis d, with no planet f nor planet g. Excluding planet f causes the predictions to spread out in period space, indicative of two planets possibly missing. Excluding planet g moves the exterior injection space to center almost directly on the period of planet g.

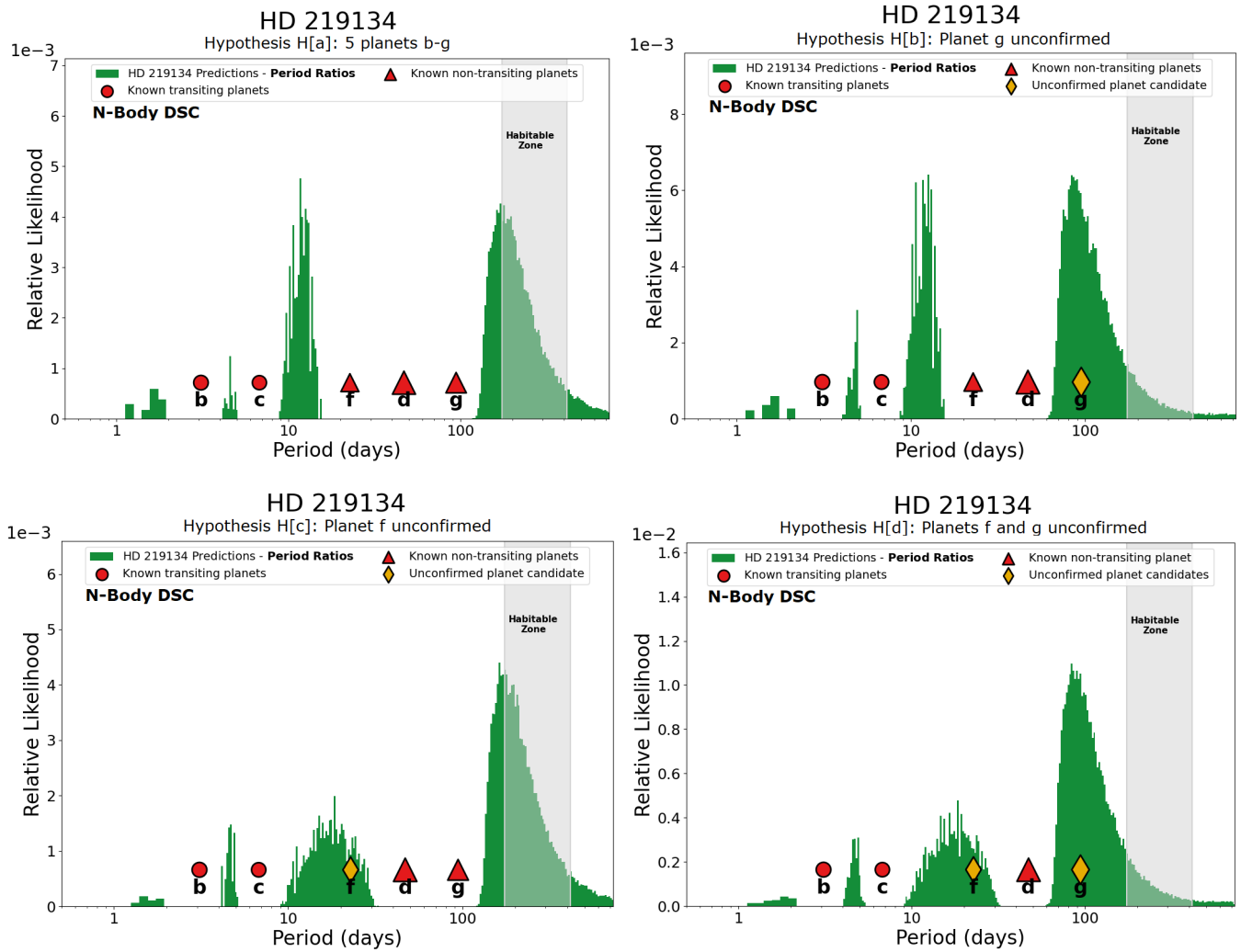


Figure 12. DYNAMITE analysis utilizing the N-body simulations and testing orbit crossing and the AMD spectral fraction. Top left: Analysis assuming full 5-planet system. Top right: Analysis assuming no planet f (orbital period near stellar rotation period). Bottom left: Analysis assuming no planet g (not found in all studies). Bottom right: Analysis assuming no planet f nor planet g. The results here are similar to the simple dynamical stability criterion, only with tighter restraints near the $\Delta = 8$ limit and at orbital resonances.